Advances in Continuous and Discrete Models

RESEARCH Open Access

Stability and bifurcation analysis of a delayed stage-structured predator–prey model with fear, additional food, and cooperative behavior in both species

Huazhou Mo[1,2] and Yuanfu Shao[1,2*]

*Correspondence:
shaoyuanfu@163.com
[1]School of Mathematics and Statistics, Guilin University of Technology, Guilin, Guangxi 541004, China
[2]Guangxi Colleges and Universities Key Laboratory of Applied Statistics, Guilin, Guangxi 541004, China

Abstract

The stability of predator–prey interactions in ecosystems is influenced by both inherent species interactions and external factors. For instance, the presence of additional food, as an external factor, may affect the system. To further explore this, a stage-structured predator–prey model is constructed, incorporating the influences of fear and delay on prey-population growth, which provides additional food for immature predators and facilitates cooperative behavior between mature and immature predators. The analysis evaluates the positivity, boundedness, equilibrium points, local stability around each equilibrium point, and certain bifurcations of the system. Additionally, numerical simulations are provided to correspond with the results of the theoretical analysis. It is observed that an appropriate level of fear contributes positively to system stability. While cooperation among predators can benefit immature predators, it also has the potential to harm the overall system. The introduction of additional food complicates the system dynamics, although it benefits predators, it places prey at a disadvantage. Furthermore, we observe a correlation between the level of fear and the effects of additional food, as well as the capacity of additional food to mitigate the influence of delay.

Keywords: Fear; Additional food; Stage structure; Cooperation; Bifurcations

1 Introduction

In the natural world, interactions among populations of different biological species form a complex ecological network that influences the structure and function of ecosystems. These interactions can include competition, predation, mutualism, and parasitism, etc. Among these relationships, the predator–prey relationship is a crucial interaction in the ecosystem. The interaction between the predator and the prey is also known as a functional response. By studying functional responses, we can gain deeper insights into the interaction patterns between predators and prey, as well as the impacts of these interactions on ecosystem structure and stability.

Initially, the classical Lotka–Volterra model posited that the growth rate of predators is directly proportional to the abundance of prey, representing a linear functional response [1, 2]. However, in real ecological systems, the predation rate does not increase indefinitely; instead, it saturates as prey abundance rises. To more accurately depict this phenomenon, researchers have introduced various saturating functional response forms. Among these, Holling proposed the classic prey-dependent functional response types: Type II and Type III [3]. Subsequently, researchers also considered predator-dependent functional responses, such as the Beddington–DeAngelis type [4]. Over the past few decades, ecologists have gradually moved beyond the classical Lotka–Volterra model in their exploration of predator–prey relationships. They have incorporated different types of functional responses into their models, taking into account a range of new influencing factors. These factors include the prey's fear effect, additional food supply in the external environment, cooperation and competition among populations, and time delays between predators and prey. Such complex factors enable researchers to simulate and understand the interactions between predators and prey in ecosystems more accurately, providing valuable insights and methods for further advancements in the field of ecology.

Fear plays a crucial role in ecology and evolutionary biology. Unlike the direct killing of prey, which leads to a reduction in population numbers, fear effects may exert broader and more prolonged impacts on prey populations by altering their behavior, life-history traits, and spatial utilization within the ecosystem, as demonstrated by numerous studies. For instance, Mao et al. [5] investigated the effects of both direct predation and fear-induced behaviors on prey populations in the ecosystems of Yellowstone National Park. They found that fear effects, such as altered grazing patterns and habitat use by herbivores in response to predation risk, had significant impacts on vegetation dynamics and ecosystem structure. Ripple et al. [6] examined the ecological cascades resulting from the reintroduction of wolves to Yellowstone National Park. By reducing elk populations through predation and fear effects, wolves indirectly facilitated the recovery of aspen and willow populations, which had been overgrazed by elk in the absence of top predators. Additionally, Zanette et al. [7] conducted a study that revealed that merely perceiving predation risk, achieved by broadcasting predator calls, could reduce the annual offspring production of songbird populations by 40%. The significant impact of fear was further acknowledged by Wang et al., who first introduced fear-mediated effects into mathematical models [8]. Their study demonstrated that fear can stabilize the prey–predator system and prevent oscillatory behavior.

Food is essential for the survival of biological populations, and consequently, the impact of supplemental food has attracted significant attention and research. Numerous studies indicate that providing additional food to biological populations can influence their behavior. For example, in Passer domesticus, the provision of extra food results in changes in female behavior, allowing mates to spend more time together in the nest, which in turn reduces the incidence of extra-pair paternity [9]. During winter, populations of Poecile atricapillus defend foraging territories; however, this system often collapses when additional food is made available [10]. Furthermore, the effects of supplemental food have been extensively examined through mathematical models [11–14]. Ghosh et al. [11] investigated the effects of supplemental food on predator–prey dynamics in scenarios where the risk of predation is low due to prey refuge. Their findings suggest that in high-prey-refuge ecological systems, providing additional food to the predator population can mitigate the risk

of predator-species extinction. Ananth et al. [14] formulated and analyzed optimal control problems aimed at achieving desired outcomes in the shortest possible time. They considered two distinct models of supplemental food and discussed the ecological implications of their theoretical findings for these models.

In ecosystems, the behavior and abilities of a species at different stages of growth and development vary. The hunting ability at different ages is related to its position and impact, and the life cycles of prey are also affected by these predators. Many studies classify the age structure of biological populations into immature and mature prey or predators [15–19]. It is common for mature individuals to provide partial care and protection to immature ones within populations. For instance, in wolf packs, caretakers frequently do not leave the pups alone but rather cooperate with other members to ensure the safety and survival of the immature [20]. Additionally, wolf packs often collaborate to hunt prey that is much larger than themselves [21]. This form of intracooperation was investigated by the author in [22], who introduced predator cooperation into the Holling Type-II functional response within the model, analyzing stability and various bifurcation types. The study concluded that the absence of cooperation among predators renders the system highly sensitive. Vishwakarma and Sen [23] explored how predator cooperation and Allee effects influence the system, observing that the introduction of cooperation adds complexity to the dynamics. Research on population cooperation is also discussed in [24–29] and other literature.

On the other hand, various relationships and interactions within an ecological system often exhibit time delays. For instance, when an organism experiences a fear stimulus, its response to subsequent stimuli not only persists beyond the cessation of the initial stimulus but may also endure for a period following a delay. Considering the presence of these delays brings us closer to reality, and extensive investigations have been conducted into how delayed fear responses impact population dynamics systems [30–33]. Ramasamy et al. [30] explored the incorporation of fear delay in an intermediate predator and the provision of additional food for the top predator within a three-species food chain. Their study found that the chaotic dynamics of the model could be controlled by appropriately selecting parameters related to the fear effect and the provision of additional food. Sui and Du [33] conducted an analysis within a diffusive predator–prey model, examining three distinct scenarios regarding the impact of fear-response delay on prey reproduction. Additionally, there may be other delays, such as gestation [34], digestion [35], and disease transmission [36] delays.

Inspired by the analysis presented above, this article aims to develop an age-structured predator–prey system that incorporates factors such as fear, additional food resources, and intrapopulation cooperation. We will explore how these elements influence the stability of the system.

The organization of this paper is structured as follows: Sect. 2 presents the model construction. Section 3 evaluates and analyzes the positivity, boundedness, equilibrium points, as well as the local stability and bifurcations of the system. In Sect. 4, we conduct numerical simulations of the system. Finally, Sect. 5 provides a summary and offers perspectives for future work.

2 Model formulation

In this section, we formulate a three-species model that includes one prey species (x) and two predator species at different stage structures. One is referred to as adult predator (y_1),

and the other is referred to as immature predator (y_2). To construct our model, we will proceed with the following steps and provide relevant assumptions for explanation.

(1). Let us consider the hypothetical scenario where the prey population grows logically in the absence of any predator or predation-related concerns. The logistic growth function is dependent on two environmental parameters, namely the intrinsic growth rate and carrying capacity of the prey population. Based on this assumption, we derive the following ordinary differential equation:

$$\frac{dx}{dt} = rx\left(1 - \frac{x}{V}\right).$$

(2). Furthermore, the presence of predators induced predation fear in the prey. We assume that the fear of predation diminishes the inherent growth rate of the prey. To incorporate this effect into the aforementioned model equation, we modify it by multiplying the intrinsic growth rate of the prey by a monotonically decreasing function denoted as $g(y_1, y_2, k) = e^{-k(y_1+y_2)}$ (refer to [37]). By incorporating the fear factor into the prey-growth birth rate, a decrease in the fear function value, specifically observed when the predator biomass is higher, leads to a corresponding reduction in the birth rate of the prey. Apart from the indirect influence of predators on prey through fear, the indirect interaction between adult predators and prey is assumed to follow the Beddington–DeAngelis-type functional response and between immature predators and prey obey the Holling Type-II functional response. Additionally, we hypothesize a behavior within the predator population where adults may protect and care for immatures, ensuring the survival and reproduction of the group. This behavior contributes to increased overall survival success of the group and helps shield immatures from harm. As a result, the model is obtained as follows:

$$\begin{cases} \dfrac{dx}{dt} = rxe^{-k(y_1+y_2)}\left(1 - \dfrac{x}{V}\right) - d_1x - \dfrac{s_1xy_1}{1+x+y_1} - \dfrac{s_2xy_2}{1+x}, \\ \dfrac{dy_1}{dt} = \dfrac{\varpi_1 s_1 xy_1}{1+x+y_1} - d_2y_1 - cy_1^2 + \sigma y_2, \\ \dfrac{dy_2}{dt} = \dfrac{\varpi_2 s_2 xy_2}{1+x} + \delta y_1y_2 - \sigma y_2. \end{cases} \tag{2.1}$$

The effect of protection by the mature predator to the immature predator is indicted by the term δy_1y_2 (more details can be found in [29]).

(3). To alleviate food scarcity, predator is supplemented with an additional food of quantity B, which is uniformly distributed throughout the habitat. We assume that the encounters with additional food per predator is directly proportional to the density of the supplemental food, meaning that each predator's exposure to extra food is proportional to the availability of such food in the area. This additional food biomass causes changes in the functional response of predators. Then, (2.1) has

Table 1 Biological implications of parameters in the system (2.3)

Coefficient	Biological explanation	Dimension
x	Prey	*biomass*
y_1	Adult predator	*biomass*
y_2	Immature predator	*biomass*
r	Prey intrinsic growth rate	$time^{-1}$
V	The carrying capacity of the environment for prey	*biomass*
s_1	The predation rate of adult predator	$time^{-1}$
s_2	The predation rate of immature predator	$time^{-1}$
k	Level of fear effect	$biomass^{-1}$
ρ	Conversion rate of additional food	–
α	Effectual food rate	–
B	Quantity of additional food	*biomass*
c	Intraspecific competition coefficient of adult predator	$biomass^{-1}\,time^{-1}$
σ	Adult rate of immature predator	$time^{-1}$
ϖ_1	Conversion rate of prey to adult predator	*biomass*
ϖ_2	Conversion rate of prey to immature predator	*biomass*
δ	Cooperation between mature and immature prey	$time^{-1}$
d_1	Natural mortality rate of prey	$time^{-1}$
d_2	Natural mortality rate of adult predator	$time^{-1}$

been modified as follows:

$$\begin{cases} \dfrac{dx}{dt} = rxe^{-k(y_1+y_2)}\left(1-\dfrac{x}{V}\right) - d_1x - \dfrac{s_1xy_1}{1+x+y_1} - \dfrac{s_2xy_2}{1+\rho\alpha B+x}, \\ \dfrac{dy_1}{dt} = \dfrac{\varpi_1 s_1 xy_1}{1+x+y_1} - d_2y_1 - cy_1^2 + \sigma y_2, \\ \dfrac{dy_2}{dt} = \dfrac{\varpi_2 s_2(x+\alpha B)y_2}{1+\rho\alpha B+x} + \delta y_1y_2 - \sigma y_2. \end{cases} \tag{2.2}$$

The term $\frac{\varpi_1 s_1(x+\alpha B)y}{1+x+\rho\alpha B}$ represents the functional response after providing additional food, a relevant biological explanation is mentioned in reference [38].

(4). In real biological systems, the growth or decline of population numbers may be subject to certain delayed effects, which may be caused by intrinsic biological factors or environmental influences. This delay effect can have an impact on population dynamics. Based on these considerations, we introduce time delays in the system (2.2) as follows:

$$\begin{cases} \dfrac{dx}{dt} = rxe^{[-k(y_1+y_2)(t-\tau)]}\left(1-\dfrac{x}{V}\right) - d_1x - \dfrac{s_1xy_1}{1+x+y_1} - \dfrac{s_2xy_2}{1+\rho\alpha B+x}, \\ \dfrac{dy_1}{dt} = \dfrac{\varpi_1 s_1 xy_1}{1+x+y_1} - d_2y_1 - cy_1^2 + \sigma y_2, \\ \dfrac{dy_2}{dt} = \dfrac{\varpi_2 s_2(x+\alpha B)y_2}{1+\rho\alpha B+x} + \delta y_1y_2 - \sigma y_2, \end{cases} \tag{2.3}$$

where τ is regarded as prey's fear that results in a time delay in the intrinsic growth of prey. The biological meanings associated with the parameters of the system (2.3) and the interactions between organisms are presented in Table 1 and Fig. 1.

The initial conditions are:

$$x(\varsigma) = \psi_1(\varsigma),\ y_1(\varsigma) = \psi_2(\varsigma),\ y_2(\varsigma) = \psi_3(\varsigma),\ -\tau \le \varsigma \le 0, \tag{2.4}$$

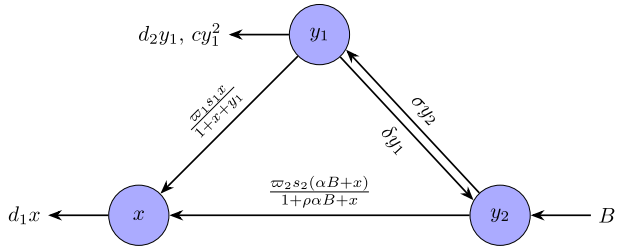

Figure 1 Schematic diagram illustrating the interactions among prey (x), adult predator (y_1), and immature predator (y_2)

where $\psi_i(\varsigma) \geq 0\,(i = 1,2,3)$ denotes any continuous function mapping from $[-\tau, 0]$ into $R_+ = [0,\infty]$ with $||\psi|| = \sup_{[-\tau,0]} \{|\psi_1(\varsigma)|, |\psi_2(\varsigma)|, |\psi_3(\varsigma)|\}$.

3 System evaluation and analysis

Let us start by summarizing some fundamental dynamical properties of the system, including its positivity, boundedness, and persistence.

3.1 Positiveness and boundedness of the solutions

Theorem 1 *All solutions of the system* (2.3) *with initial conditions* (2.4) *are positive for all* $t > 0$.

Proof For the purposes of analytical tractability, we let:

$$\begin{cases} F_1(x,y_1,y_2) = re^{[-k(y_1+y_2)(t-\tau)]}\left(1-\frac{x}{V}\right) \\ \qquad\qquad -d_1 - \frac{s_1 y_1}{1+x+y_1} - \frac{s_2 y_2}{1+\rho\alpha B+x}, \\ F_2(x,y_1,y_2) = \frac{\varpi_1 s_1 x}{1+x+y_1} - d_2 - cy_1 + \sigma\frac{y_2}{y_1}, \\ F_3(x,y_1,y_2) = \frac{\varpi_2 s_2(x+\alpha B)}{1+\rho\alpha B+x} + \delta y_1 - \sigma. \end{cases}$$

Then, we rewrite the system (2.3) as:

$$\frac{dx}{dt} = xF_1(x,y_1,y_2), \quad \frac{dy_1}{dt} = y_1F_2(x,y_1,y_2), \quad \frac{dy_2}{dt} = y_2F_3(x,y_1,y_2).$$

By using Lemma 4 given in [39] and the initial conditions (2.4), we have:

$$x(t) \geq x(0)\exp\left\{\int_0^t \left[F_1(x(\nu),y_1(\nu),y_2(\nu)) - d\nu)\right]d\nu\right\} > 0,$$
$$y_1(t) \geq y_1(0)\exp\left\{\int_0^t [F_2(x(\nu),y_1(\nu),y_2(\nu)) - d\nu]d\nu\right\} > 0,$$
$$y_2(t) \geq y_2(0)\exp\left\{\int_0^t [F_3(x(\nu),y_1(\nu),y_2(\nu)) - d\nu]d\nu\right\} > 0.$$

We obtain that every solution of the system (2.3) is positive and invariant for all $t > 0$. □

Theorem 2 *All solutions of the system remain uniformly bounded under the initial conditions* (2.4) *for all* $t > 0$.

Proof Since, $\frac{dx}{dt} \le rxe^{-k(y_1+y_2)}\left(1-\frac{x}{V}\right) \le rx\left(1-\frac{x}{V}\right)$, applying the comparison principle, we obtain:

$$\limsup_{t\to 0} x \le \frac{r}{r/V} = V \Rightarrow x_{\max} = V.$$

Let $w(t) = x + \frac{1}{\varpi_1}y_1(t) + \frac{1}{\varpi_1}y_2(t)$, then calculate the derivative of $w(t)$ along the solution of the system (2.2), we have:

$$\begin{aligned}
\frac{dw}{dt} &= \frac{dx}{dt} + \frac{1}{\varpi_1}\frac{dy_1}{dt} + \frac{1}{\varpi_2}\frac{dy_2}{dt} \\
&= rxe^{-k(y_1+y_2)}\left(1-\frac{x}{V}\right) - d_1x + \frac{s_2\alpha B}{1+\rho\alpha B+x}y_2 - \frac{d_2}{\varpi_1}y_1 - \frac{c}{\varpi_1}y_1^2 \\
&\qquad + \frac{\sigma}{\varpi_1}y_2 + \frac{\delta}{\varpi_2}y_1y_2 - \frac{\sigma}{\varpi_2}y_2 \\
&\le rxe^{-k(y_1+y_2)}\left(1-\frac{x}{V}\right) - \frac{c}{\varpi_1}y_1^2 + \frac{s_2\alpha B}{1+\rho\alpha B+x}y_2 + \frac{\sigma}{\varpi_1}y_2 + \frac{\delta}{\varpi_2}y_1y_2 - \frac{\sigma}{\varpi_2}y_2 \\
&\le rV - \frac{c}{\varpi_1}y_1^2 - \frac{d_2}{\varpi_1}y_1 + s_2\alpha By_2 + \frac{\sigma}{\varpi_1}y_2 + \frac{\delta}{\varpi_2}y_1y_2 \\
&= rV - \frac{c}{\varpi_1}\left(y_1 - \frac{\varpi_1\delta}{2\varpi_2 c}y_2\right)^2 - \frac{d_2}{\varpi_1}y_1 + \frac{\varpi_1\delta^2}{4c\varpi_2^2}y_2^2 - \frac{\varpi_1 s_2\alpha B+\sigma}{\varpi_1}y_2 \\
&\le rV - \frac{d_2}{\varpi_1}y_1 + \frac{\varpi_1\delta^2}{4c\varpi_2^2}y_2^2 - \frac{\varpi_1 s_2\alpha B+\sigma}{\varpi_1}y_2.
\end{aligned}$$

For any positive ξ, we have:

$$\begin{aligned}
\frac{dw}{dt} + \xi w &\le rV + \xi x + \frac{\xi - d_2}{\varpi_1}y_1 - \frac{\varpi_1\delta^2}{4c\varpi_2^2}\left(\frac{4c\varpi_2^2(\varpi_1\varpi_2 s_2\alpha B + \varpi_2\sigma + \varpi_1\xi)}{\varpi_2\varpi_1^2\delta^2}y_2 - y_2^2\right) \\
&\le (r+\xi)V + \frac{\xi - d_2}{\varpi_1}y_1 - \frac{\varpi_1\delta^2}{4c\varpi_2^2}\left(\frac{4c\varpi_2^2(\varpi_1\varpi_2 s_2\alpha B + \varpi_2\sigma + \varpi_1\xi)}{2\varpi_2\varpi_1^2\delta^2}\right)^2 \\
&\le (r+\xi)V + \frac{\xi - d_2}{\varpi_1}y_1.
\end{aligned}$$

Choosing ξ sufficiently small satisfying $\xi < d_2$, we obtain:

$$\frac{dw}{dt} + \xi w \le (r+\xi)V = Q.$$

Considering $Q > 0$, then we can rewrite the above differential inequality as:

$$\frac{d}{dt}\left(w - \frac{Q}{\xi}\right) \le -\xi\left(w - \frac{Q}{\xi}\right).$$

By using the theory of differential inequality for $w(t)$, we obtain:

$$0 \le w(x, y_1, y_2) \le \frac{Q}{\xi} + w(0)e^{-\xi t},$$

where $w(0) = \big(x(0), y_1(0), y_2(0)\big)$, when $t \to \infty$, $0 < w \leq \frac{Q}{\xi}$. Hence, the system is uniformly bounded. □

3.2 Assessment of equilibrium

In this subsection, we will explore the existence of several distinct equilibrium points for the system (2.2). The system (2.2) always possesses a trivial equilibrium point. Under certain conditions, the system displays both predator-free and interior equilibrium points as described below.

(1) The population-free equilibrium $P_0 = (0, 0, 0)$, which always exists.

(2) The immature and adult predator-free equilibrium $P_1 = (\hat{x}, 0, 0)$, where $\hat{x} = \frac{V(r-d_1)}{r}, r > d_1$.

(3) The adult predator-free equilibrium $P_2 = (\bar{x}, 0, \bar{y}_2)$, where $\bar{x} = \frac{\sigma+\sigma\rho\alpha B-\varpi_2 s_2\alpha B}{\varpi_2 s_2-\sigma} = \wp(\bar{x}) < V$ and $\bar{y}_2$ represents the positive root of the equation shown below:

$$\mho_1 e^{-k\bar{y}_2} - \mho_2\bar{y}_2 - d_1 = 0,$$

here $\mho_1 = r\left(1 - \frac{\wp(\bar{x})}{V}\right)$ and $\mho_2 = \frac{s_2}{1+\rho\alpha B+\wp(\bar{x})}$. Let $\hbar(\bar{y}_2) = \mho_1 e^{-k\bar{y}_2} - \mho_2\bar{y}_2 - d_1$, then the derivative of $\hbar(\bar{y}_2)$ with respect to $\bar{y}_2$ yields $\hbar(\bar{y}_2)' = -k\mho_1 e^{-ky_2} - \mho_2 < 0$. When $\bar{y}_2 \to \infty$, $\lim_{\bar{y}_2\to\infty} \hbar(\bar{y}_2) < 0$ and $\bar{y}_2 \to 0$, $\lim_{\bar{y}_2\to\infty} \hbar(\bar{y}_2) > 0$ if provided $\mho_1 > d_1$. Therefore, the system possesses a unique adult predator-free equilibrium point if $\mho_1 > d_1$.

(4) The immature predator-free equilibrium $P_3 = (x^\bullet, y_1^\bullet, 0)$, where $x^\bullet$ and $y_1^\bullet$ are derived from the positive root of the following equation:

$$\begin{cases} \mathfrak{S}_1(x^\bullet, y_1^\bullet) = re^{-ky_1^\bullet}\left(1 - \frac{x^\bullet}{V}\right) - d_1 - \frac{s_1 y_1^\bullet}{1+x^\bullet+y_1^\bullet} = 0, \\ \mathfrak{S}_2(x^\bullet, y_1^\bullet) = \frac{\varpi_1 s_1 x^\bullet}{1+x^\bullet+y_1^\bullet} - d_2 - cy_1^\bullet = 0. \end{cases} \tag{3.1}$$

If the nullclines $\mathfrak{S}_1(x^\bullet, y_1^\bullet) = 0$ and $\mathfrak{S}_2(x^\bullet, y_1^\bullet) = 0$ intersect in the positive quadrant, then the immature predator-free equilibrium point can be obtained.

(5) The coexistence equilibrium $P_4 = (x^*, y_1^*, y_2^*)$ within the positive quadrant, where x^*, y_1^*, and y_2^* are the positive solution of the subsequent system of the nonlinear equations:

$$\begin{cases} re^{-k(y_1^*+y_2^*)}\left(1 - \frac{x^*}{V}\right) - d_1 - \frac{s_1 y_1^*}{1+x^*+y_1^*} - \frac{s_2 y_2^*}{1+\rho\alpha B+x^*} = 0, \\ \frac{\varpi_1 s_1 x^* y_1^*}{1+x^*+y_1^*} - d_2 y_1^* - c(y_1^*)^2 + \sigma y_2^* = 0, \\ \frac{\varpi_2 s_2(x^*+\alpha B)}{1+\rho\alpha B+x^*} + \delta y_1^* - \sigma = 0. \end{cases} \tag{3.2}$$

We can obtain the expression for y_1^* from the third equation of (3.2) as follows:

$$y_1^* = \frac{\sigma}{\delta} - \frac{\varpi_2 s_2(x^* + \alpha B)}{\delta(1 + \rho\alpha B + x^*)} = \ell(y_1^*). \tag{3.3}$$

Ensuring y_1^* is positive and substituting it into the second equation of (3.3), we obtain the relationship between x and y_2 as:

$$\begin{cases} \Phi_1(x^*, y_2^*) = re^{-k(\ell(y_1^*)+y_2^*)}\left(1-\frac{x^*}{V}\right) - d_1 \\ \qquad\qquad -\frac{s_1\ell(y_1^*)}{1+x^*+\ell(y_1^*)} - \frac{s_2 y_2^*}{1+\rho\alpha B+x^*} = 0, \\ \Phi_2(x^*, y_2^*) = \frac{\varpi_1 s_1 x^* \ell(y_1^*)}{1+x^*+\ell(y_1^*)} - d_2\ell(y_1^*) - c(\ell(y_1^*))^2 + \sigma y_2^* = 0. \end{cases} \tag{3.4}$$

If the point of intersection (x^*, y_2^*) for the nullclines $\Phi_1(x^*, y_2^*) = 0$ and $\Phi_2(x^*, y_2^*) = 0$ is found (refer to Fig. 2(a)), it allows for the determination of y_1^* through (3.2), thereby the existence of the interior equilibrium P_4 is established (refer to Fig. 2(b)).

Remark 1 Note that the equilibrium points of the system (2.2) coincide with the equilibrium points of the system (2.3). Finding explicit formulations for the positive roots of (3.1) and (3.2) is a challenging task due to their nonlinear nature. We will calculate the equilibrium points by taking specific parameter values during the numerical simulations in Sect. 4.

3.3 Stability and bifurcation analysis near equilibria

In this section, we investigate the local stability and bifurcation of the system around its equilibrium points. The local stability of each equilibrium point can be studied using the theory of Jacobian matrices.

3.3.1 No delay case

(1) Dynamics near $\boldsymbol{P_0}$

The Jacobian matrix J_{p_0} at $P_0(0,0,0)$ is given by:

$$J_{P_0} = \begin{pmatrix} r-d_1 & 0 & 0 \\ 0 & -d_2 & \sigma \\ 0 & 0 & \frac{\varpi_2 s_2 \alpha B}{1+\rho\alpha B} - \sigma \end{pmatrix}.$$

The characteristic equation for the system (2.2) at trivial equilibrium P_0 is:

$$(r-d_1-\lambda)(-d_2-\lambda)\left(\frac{\varpi_2 s_2 \alpha B}{1+\rho\alpha B} - \sigma - \lambda\right) = 0. \tag{3.5}$$

Among the roots of Eq. (3.5), one of them is a negative real number $\lambda_1 = -d_2$, the other two roots are $\lambda_2 = r - d_1$ and $\lambda_3 = \frac{\varpi_2 s_2 \alpha B}{1+\rho\alpha B} - \sigma$. Now, if $r < d_1$ and $\varpi_2 s_2 \alpha B < \sigma + \sigma\rho\alpha B$ then all characteristic roots are negative real numbers. Therefore, the following theorem can be derived:

Theorem 3 *The trivial equilibrium point $P_0(0,0,0)$ is locally asymptotically stable if $r < d_1$ and $\varpi_2 s_2 \alpha B < \sigma + \sigma\rho\alpha B$, otherwise, it demonstrates unstable dynamics.*

(2) Dynamics near $\boldsymbol{P_1}$

The Jacobian matrix for the system (2.2) at $P_1(\hat{x},0,0)$ is given by

$$J_{P_1}=\begin{pmatrix} A_{11} & A_{12} & A_{13} \\ 0 & A_{22} & \sigma \\ 0 & 0 & A_{33} \end{pmatrix},$$

where

$$A_{11}=r\left(1-\frac{\hat{x}}{V}\right)-d_1-\frac{r\hat{x}}{V}<0, A_{12}=-kr\hat{x}\left(1-\frac{x}{V}\right)-\frac{s_1\hat{x}}{1+\hat{x}},$$
$$A_{13}=-kr\hat{x}\left(1-\frac{\hat{x}}{V}\right)-\frac{s_2\hat{x}}{1+\rho\alpha B+\hat{x}}, A_{22}=\frac{\varpi_1 s_1\hat{x}}{1+\hat{x}}-d_2, A_{33}=\frac{\varpi_2 s_2(\hat{x}+\alpha B)}{1+\rho\alpha B+\hat{x}}-\sigma.$$

The characteristic equation of the system (2.2) at the equilibrium point $P_1(\hat{x},0,0)$ is

$$(A_{11}-\lambda)(A_{22}-\lambda)(A_{33}-\lambda)=0. \tag{3.6}$$

It is easy to determine that one of the roots of Eq. (3.6) is $\lambda_1=A_{11}<0$. If the other two characteristic roots, $\lambda_2=A_{22}$ and $\lambda_3=A_{33}$ are also negative, then it is possible to judge the local stability near the equilibrium point P_1 (see Theorem 4).

Theorem 4 *The equilibrium P_1 is locally asymptotically stable if $\varpi_1 s_1\hat{x}<d_2+\hat{x}$ and $\varpi_1 s_1(\hat{x}+\alpha B)<\sigma+\sigma\rho\alpha B+\sigma\hat{x}$.*

(3) Dynamics near P_2

The Jacobian matrix for the system (2.2) at $P_2=(\bar{x},0,\bar{y}_2)$ is given by

$$J_{P_2}=\begin{pmatrix} \Gamma_{11} & \Gamma_{12} & \Gamma_{13} \\ 0 & \Gamma_{22} & \Gamma_{23} \\ \Gamma_{31} & \Gamma_{23} & \Gamma_{33} \end{pmatrix},$$

where

$$\Gamma_{11}=re^{-k\bar{y}_2}\left(1-\frac{2\bar{x}}{V}\right)-d_1-\frac{s_2\bar{y}_2(1+\rho\alpha B)}{(1+\rho\alpha B+\bar{x})^2}, \Gamma_{12}=-kr\bar{x}e^{-k\bar{y}_2}\left(1-\frac{\bar{x}}{V}\right)-\frac{s_1\bar{x}}{1+\bar{x}},$$
$$\Gamma_{13}=-kr\bar{x}e^{-k\bar{y}_2}\left(1-\frac{\bar{x}}{V}\right)-\frac{s_2\bar{x}}{1+\rho\alpha B+\bar{x}}, \Gamma_{22}=\frac{\varpi_1 s_1\bar{x}}{1+\bar{x}}-d_2, \Gamma_{23}=\sigma, \Gamma_{32}=\delta\bar{y}_2,$$
$$\Gamma_{31}=\frac{\varpi_2 s_2\bar{y}_2(1+\rho\alpha B-\alpha B)}{(1+\rho\alpha B+\bar{x})^2}, \Gamma_{33}=\frac{\varpi_2 s_2(\bar{x}+\alpha B)}{1+\rho\alpha B+\bar{x}}-\sigma.$$

Calculating the characteristic equation based on the Jacobian matrix as shown in (3.7):

$$\lambda^3+\Re_1\lambda^2+\lambda\Re_2+\Re_3=0, \tag{3.7}$$

where

$$\Re_1=-\Gamma_{11}-\Gamma_{22}-\Gamma_{33}, \Re_2=\Gamma_{33}\Gamma_{11}+\Gamma_{33}\Gamma_{22}+\Gamma_{11}\Gamma_{22}-\Gamma_{31}\Gamma_{13}-\Gamma_{22}\Gamma_{23}$$
$$\Re_3=\Gamma_{31}\Gamma_{22}\Gamma_{13}+\Gamma_{11}\Gamma_{22}\Gamma_{23}-\Gamma_{11}\Gamma_{22}\Gamma_{33}-\Gamma_{31}\Gamma_{22}\Gamma_{12}.$$

Assuming conditions $\Re_1 > 0$, $\Re_3 > 0$, and $\Re_1\Re_2 > \Re_3$ are satisfied, then according to the Routh–Hurwitz criterion, it is known that all roots of (3.7) are negative. This implies that P_2 is locally asymptotically stable near the system (2.2). Now, we take the parameter k as the bifurcation parameter and ensure that k satisfies: $\Re_1(k^H)\Re_2(k^H) = \Re_3(k)$, so Eq. (3.7) transforms into:

$$(\lambda^2 + \Re_2)(\lambda + \Re_1) = 0. \tag{3.8}$$

It is evident that the roots of Eq. (3.8) include one real root $\lambda_1 = -\Re_1$ and two imaginary roots $\lambda_{2,3} = \pm i\sqrt{\Re_2}$. Let the form of the roots of (3.8) be $\lambda = \varphi(k) \pm i\beta(k)$, and substituting into (3.8) yields:

$$(\varphi(k) + i\beta(k))^3 + \Re_1(\varphi(k) + i\beta(k))^2 + \Re_2(\varphi(k) + i\beta(k)) + \Re_3 = 0. \tag{3.9}$$

Differentiate (3.9) with respect to k and separate the real and imaginary parts, then

$$\Im_1(k)\frac{\partial\varphi}{\partial k} - \Im_2(k)\frac{\partial\beta}{\partial k} = \Omega_1(k), \quad \Im_2(k)\frac{\partial\varphi}{\partial k} + \Im_1(k)\frac{\partial\beta}{\partial k} = \Omega_2(k), \tag{3.10}$$

where

$$\Im_1 = 3\varphi^2 - 3\beta^2 + 2\Re_1\varphi + \Re_2, \quad \Im_2 = 6\varphi\beta + 2\Re_1\beta,$$
$$\Omega_1 = \beta^2\frac{\partial\Re_1}{\partial k} - \varphi^2\frac{\partial\Re_1}{\partial k} - \varphi\frac{\partial\Re_2}{\partial k} - \frac{\partial\Re_3}{\partial k}, \quad \Omega_2 = 2\varphi\beta\frac{\partial\Re_1}{\partial k} + \beta\frac{\partial\Re_2}{\partial k}.$$

Observing that $\varphi(k^H) = 0$ and $\beta(k^H) = \sqrt{\Re_2}$, we have:

$$\Im_1 = -2\Re_2, \ \Im_2 = 2\Re_1\sqrt{\Re_2}, \ \Omega_1 = \Re_2\frac{\partial\Re_1}{\partial k} - \frac{\partial\Re_3}{\partial k}, \ \Omega_2 = \frac{\partial\Re_2}{\partial k}\sqrt{\Re_2}.$$

Checking whether the transversality condition holds, by isolating from (3.10) we have

$$\frac{\partial}{\partial k}(\mathrm{Re}\lambda(k))\bigg|_{k=k^H} = \frac{\Im_1\Omega_1 + \Im_2\Omega_2}{\Im_1^2 + \Im_2^2} \neq 0, \text{if } \Im_1\Omega_1 + \Im_2\Omega_2 \neq 0 \text{ and } \lambda_1 = -\Re_1 \neq 0.$$

If the condition holds, a Hopf bifurcation occurs around P_2 at $k = k^H$.

Theorem 5 *The system* (2.2) *is locally asymptotically stable around adult predator-free equilibrium* $P_2 = (\bar{x}, 0, \bar{y}_2)$ *if conditions* $\Re_1 > 0, \Re_3 > 0$ *and* $\Re_1\Re_2 > \Re_3$ *are satisfied, then a Hopf bifurcation occurs around* P_2 *at* $k = k^H$ *such that* $\Re_1\Re_2 = \Re_3$, *provided* $\Im_1\Omega_1 + \Im_2\Omega_2 \neq 0$.

(4) Dynamics near $\boldsymbol{P_3}$

The Jacobian matrix for the system (2.2) at $P_3(x^\bullet, y_1^\bullet, 0)$ is given by

$$J_{P_3} = \begin{pmatrix} C_{11} & C_{12} & C_{13} \\ C_{21} & C_{22} & C_{23} \\ 0 & 0 & C_{33} \end{pmatrix},$$

where

$$C_{11} = -\frac{x^\bullet}{V} re^{-ky_1^\bullet} + \frac{s_1 y_1^\bullet}{1 + x^\bullet + y_1^\bullet} - \frac{s_1 y_1^\bullet (1 + y_1^\bullet)}{(1 + x^\bullet + y_1^\bullet)^2},$$

$$C_{12} = -krx^\bullet e^{-ky_1^\bullet} \left(1 - \frac{x^\bullet}{V}\right) - \frac{s_1 x^\bullet (1 + x^\bullet)}{(1 + x^\bullet + y_1^\bullet)^2},$$

$$C_{13} = -krx^\bullet e^{-ky_1^\bullet} \left(1 - \frac{x^\bullet}{V}\right) - \frac{s_2 x^\bullet}{1 + \rho\alpha B + x^\bullet},$$

$$C_{21} = \frac{\varpi_1 s_1 y_1^\bullet (1 + y_1^\bullet)}{(1 + x^\bullet + y_1^\bullet)^2}, C_{22} = \frac{\varpi_1 s_1 x^\bullet (1 + x^\bullet)}{(1 + x^\bullet + y_1^\bullet)^2} - d_2 - 2cy_1^\bullet,$$

$$C_{23} = \sigma, C_{33} = \frac{\varpi_2 s_2 (x^\bullet + \alpha B)}{1 + \rho\alpha B + x^\bullet} + \delta y_1^\bullet - \sigma.$$

We can obtain the following characteristic equation:

$$(C_{33} - \lambda)(\lambda^2 - (C_{11} + C_{22})\lambda + C_{11}C_{22} - C_{12}C_{21}) = 0. \tag{3.11}$$

One of the roots of the characteristic equation (3.11) is $\lambda_1 = C_{33}$, while the other two roots depend on equation (3.12):

$$\lambda^2 - (C_{11} + C_{22})\lambda + C_{11}C_{22} - C_{12}C_{21} = 0. \tag{3.12}$$

From the theory of roots and coefficients of quadratic equations, it is known that if the conditions $C_{11} + C_{22} < 0$ and $C_{11}C_{22} - C_{12}C_{21} < 0$ are satisfied, then equation (3.12) has two negative roots. Therefore, we can summarize Theorem 6 as follows:

Theorem 6 *The immature predator-free equilibrium* $P_3(x^\bullet, y_1^\bullet, 0)$ *is locally asymptotically stable under the conditions* $C_{33} < 0$, $C_{11}C_{22} < C_{12}C_{21}$, *and* $C_{11} + C_{22} < 0$ (C_{ij}, *i or j* $= 1, 2, 3$ *see above*).

Assuming the conditions $C_{33} < 0$ and $C_{11}C_{22} < C_{12}C_{21}$ hold, if $C_{11} + C_{22} = 0$, then Eq. (3.11) has two imaginary roots $\lambda_{1,2} = \pm i\sqrt{C_{11}C_{22} - C_{12}C_{21}}$. We can rewrite the roots of the Eq. (3.11) considering k as a bifurcation parameter as $\lambda_{1,2}(k) = \varphi(k) \pm i\beta(k)$. Substituting it into Eq. (3.12) and isolating the real and imaginary components yields:

$$\varphi^2 - \beta^2 - (C_{11}+C_{22})\varphi + C_{11}C_{22} - C_{12}C_{21} = 0, \quad 2\varphi\beta - (C_{11}+C_{22})\beta = 0. \tag{3.13}$$

Differentiating both sides of (3.13) with respect to k results in:

$$D_1 \frac{\partial \varphi}{\partial k} - D_2 \frac{\partial \beta}{\partial k} = \Sigma_1, \quad D_2 \frac{\partial \varphi}{\partial k} + D_1 \frac{\partial \beta}{\partial k} = \Sigma_2, \tag{3.14}$$

where $D_1 = 2\varphi - (C_{11} + C_{22})$, $D_2 = 2\beta$, $\Sigma_1 = \varphi\left(\frac{\partial C_{11}}{\partial k} + \frac{\partial C_{22}}{\partial k}\right) + C_{12}\frac{\partial C_{21}}{\partial k} + C_{21}\frac{\partial C_{12}}{\partial k} - C_{11}\frac{\partial C_{22}}{\partial k} - C_{22}\frac{\partial C_{11}}{\partial k}$, $\Sigma_2 = \beta\left(\frac{\partial C_{11}}{\partial k} + \frac{\partial C_{22}}{\partial k}\right)$. Noting that, at $k = k^H$, $\varphi(k^H) = 0$, $\beta(k^H) = \beta \neq 0$ and $C_{11} + C_{22} = 0$. Hence, the transversality condition can be derived from (3.14):

$$\frac{\partial}{\partial k}\left(\mathrm{Re}\lambda_{1,2}(k)\right)\Big|_{k=k^H} = \frac{\partial \varphi}{\partial k}\Big|_{k=k^H} = \frac{\Sigma_1 D_1 + \Sigma_2 D_2}{D_1^2 + D_2^2} = \frac{2r\beta^2 y_1^\bullet x^\bullet}{V} e^{-ky_1^\bullet} \neq 0.$$

According to the Hopf bifurcation theory, it is known that the system (2.2) undergoes a Hopf bifurcation around P_2, which is summarized in Theorem 7.

Theorem 7 *The system* (2.2) *undergoes a Hopf bifurcation around the immature predator-free equilibrium* P_3 *at* $k = k^H$ *staisfying*:

$$-\frac{x^\bullet}{V}re^{-ky_1^\bullet} + \frac{s_1y_1^\bullet}{1+x^\bullet+y_1^\bullet} - \frac{s_1y_1^\bullet(1+y_1^\bullet)}{(1+x+y_1^\bullet)^2} + \frac{\varpi_1s_1x^\bullet(1+x^\bullet)}{(1+x^\bullet+y_1^\bullet)^2} - d_2 - 2cy_1^\bullet = 0.$$

Now, turning our attention to other types of bifurcations near P_3. If $C_{33} = 0$ or $C_{11}C_{22} = C_{12}C_{21}$, then (3.11) has a zero eigenvalue, which may indicate the existence of bifurcation. To validate our hypothesis, we analyze using Sotomayor's theorem [40]. Take σ as a bifurcation parameter and ensure that $C_{33}(\sigma) = 0$ and $C_{11}C_{22} - C_{12}C_{21} \neq 0$ is satisfied, then there is a zero eigenvalue present in (3.11), the associated eigenvectors of J_{P_3} and $J_{P_3}^T$ are determined as: $\mathrm{Z}_1 = \begin{pmatrix} \varrho_1 & \varrho_2 & 1 \end{pmatrix}^T$ and $\mathrm{Z}_2 = \begin{pmatrix} 0 & 0 & 1 \end{pmatrix}^T$, where $\varrho_1 = \frac{C_{12}}{C_{11}}\left(\frac{C_{11}C_{23}-C_{12}C_{21}}{C_{11}C_{22}-C_{12}C_{21}}\right) - \frac{C_{13}}{C_{11}}$ and $\varrho_2 = -\frac{C_{11}C_{23}-C_{12}C_{21}}{C_{11}C_{22}-C_{12}C_{21}}$. Next, we proceed to examine the conditions required for the bifurcation.

$$(i)\ \mathrm{Z}_2^T\Lambda_\sigma\left(P_3, \sigma = \sigma^S\right) = \begin{pmatrix} 0 & 0 & 1 \end{pmatrix}\begin{pmatrix} 0 \\ 0 \\ 0 \end{pmatrix} = 0,$$

$$\text{where, } \Lambda = \begin{pmatrix} f_1 \\ f_2 \\ f_3 \end{pmatrix} = \begin{pmatrix} rxe^{-k(y_1+y_2)}\left(1-\frac{x}{V}\right) - d_1x - \frac{s_1xy_1}{1+x+y_1} - \frac{s_2xy_2}{1+\rho\alpha B+x} \\ \frac{\varpi_1s_1xy_1}{1+x+y_1} - d_2y_1 - cy_1^2 + \sigma y_2 \\ \frac{\varpi_2s_2(x+\alpha B)y_2}{1+\rho\alpha B+x} + \delta y_1y_2 - \sigma y_2 \end{pmatrix}.$$

$$(ii)\ \mathrm{Z}_2^T\left[D\Lambda_\sigma\left(P_3, \sigma = \sigma^S\right)\mathrm{Z}_1\right] = \begin{pmatrix} 0 & 0 & 1 \end{pmatrix}\left[\begin{pmatrix} 0 & 0 & 0 \\ 0 & 0 & 1 \\ 0 & 0 & -1 \end{pmatrix}\begin{pmatrix} \varrho_1 \\ \varrho_2 \\ 1 \end{pmatrix}\right] = -1 \neq 0.$$

$$\begin{aligned}(iii)\ & Z_2^T[D^2H_\sigma(P_3, \sigma = \sigma^S)(Z_1, Z_1)] \\ &= \frac{\partial^2 f_3}{\partial x\partial y_2}\varrho_1 + \frac{\partial^2 f_3}{\partial y_1\partial y_2}\varrho_2 + \frac{\partial^2 f_3}{\partial y_2\partial x} + \frac{\partial^2 f_3}{\partial y_2\partial y_1}\varrho_1 \\ &= \frac{\varpi_2s_2(1+\rho\alpha B-\alpha B)(1+\varrho_1)}{(1+\rho\alpha B+x^\bullet)^2} + \delta(\varrho_1+\varrho_2) = \mathcal{O},\end{aligned}$$

where,

$$D^2H = \begin{pmatrix} \frac{\partial^2 f_1}{\partial x\partial x} & \frac{\partial^2 f_1}{\partial x\partial y_1} & \frac{\partial^2 f_1}{\partial x\partial y_2} & \frac{\partial^2 f_1}{\partial y_1\partial x} & \frac{\partial^2 f_1}{\partial y_1\partial y_1} & \frac{\partial^2 f_1}{\partial y_1\partial y_2} & \frac{\partial^2 f_1}{\partial y_2\partial x} & \frac{\partial^2 f_1}{\partial y_2\partial y_1} & \frac{\partial^2 f_1}{\partial y_2\partial y_2} \\ \frac{\partial^2 f_2}{\partial x\partial x} & \frac{\partial^2 f_2}{\partial x\partial y_1} & \frac{\partial^2 f_2}{\partial x\partial y_2} & \frac{\partial^2 f_2}{\partial y_1\partial x} & \frac{\partial^2 f_2}{\partial y_1\partial y_1} & \frac{\partial^2 f_2}{\partial y_1\partial y_2} & \frac{\partial^2 f_2}{\partial y_2\partial x} & \frac{\partial^2 f_2}{\partial y_2\partial y_1} & \frac{\partial^2 f_2}{\partial y_2\partial y_2} \\ \frac{\partial^2 f_3}{\partial x\partial x} & \frac{\partial^2 f_3}{\partial x\partial y_1} & \frac{\partial^2 f_3}{\partial x\partial y_2} & \frac{\partial^2 f_3}{\partial y_1\partial x} & \frac{\partial^2 f_3}{\partial y_1\partial y_1} & \frac{\partial^2 f_3}{\partial y_1\partial y_2} & \frac{\partial^2 f_3}{\partial y_2\partial x} & \frac{\partial^2 f_3}{\partial y_2\partial y_1} & \frac{\partial^2 f_3}{\partial y_2\partial y_2} \end{pmatrix},$$

$$(Z_1, Z_1) = \begin{pmatrix} \varrho_1^2 & \varrho_1\varrho_2 & \varrho_1 & \varrho_2^2 & \varrho_1\varrho_2 & \varrho_2 & 1 & \varrho_1 & \varrho_2 \end{pmatrix}^T.$$

According to Sotomayor's theorem, the system (2.2) undergoes a transcritical bifurcation near $P_2(x^\bullet, y_1^\bullet, 0)$ at $\sigma = \sigma^S$ provided $\mathcal{O} \neq 0$.

Theorem 8 *The system* (2.2) *undergoes a transcritical bifurcation around the immature predator-free equilibrium* $P_3(x^\bullet, y_1^\bullet, 0)$ *at* $\sigma = \sigma^S$ *given that* $\mathcal{O} \neq 0$.

Remark 2 Apart from considering σ as the bifurcation parameter around equilibrium P_3, we can also select B such that $C_{33}(B) = 0$ and $C_{11}C_{22} - C_{12}C_{21} \neq 0$, or use k as the bifurcation parameter and make $C_{11}(k)C_{22}(k) - C_{12}(k)C_{21}(k) = 0$ and $C_{33} \neq 0$. The analytical process is similar to σ, which we demonstrate in the numerical simulations presented in Sect. 4.

(5) Dynamics near $\boldsymbol{P_4}$

The Jacobian matrix at the internal equilibrium point P_3 is listed as follows:

$$J_{P_4} = \begin{pmatrix} D_{11} & D_{12} & D_{13} \\ D_{21} & D_{22} & D_{23} \\ D_{31} & D_{32} & 0 \end{pmatrix},$$

where

$$\begin{aligned}
D_{11} &= re^{-k(y_1^*+y_2^*)}\left(1-\frac{2x^*}{V}\right) - d_1 - \frac{s_1 y_1^*(1+y_1^*)}{(1+x^*+y_1^*)^2} - \frac{s_2 y_1^*(1+\rho\alpha B)}{(1+\rho\alpha B+x^*)^2}, \\
D_{12} &= -kd_1x^* - \frac{ks_1x^*y_1^*}{1+x^*+y_1^*} - \frac{ks_2x^*y_2^*}{1+\rho\alpha B+x^*} - \frac{s_1x^*(1+x^*)}{(1+x+y_1^*)^2}, \\
D_{13} &= -kd_1x^* - \frac{ks_1x^*y_1^*}{1+x^*+y_1^*} - \frac{ks_2x^*y_2^*}{1+\rho\alpha B+x^*} - \frac{s_2x^*}{1+\rho\alpha B+x^*}, \\
D_{21} &= \frac{\varpi_1 s_1 y_1^*(1+y_1^*)}{(1+x^*+y_1^*)^2}, D_{22} = \frac{\varpi_1 s_1 x^*(1+x^*)}{(1+x^*+y_1^*)^2} - d_2 - 2cy_1^*, \\
D_{23} &= \sigma, D_{31} = \frac{\varpi_2 s_2 y_2^*(1+\rho\alpha B-\alpha B)}{(1+\rho\alpha B+x^*)^2}, D_{32} = \delta y_2^*.
\end{aligned}$$

The characteristic equation at the internal equilibrium point P_3 is

$$\lambda^3 + L_1\lambda^2 + L_2\lambda + L_3 = 0, \tag{3.15}$$

where $L_1 = -D_{11} - D_{22}$, $L_2 = D_{11}D_{22} - D_{13}D_{31} - D_{23}D_{32}$, $L_3 = D_{23}D_{32}D_{11} + D_{13}D_{31}D_{22} - D_{12}D_{23}D_{31} - D_{21}D_{32}D_{13}$. Clearly, if $L_1 > 0, L_3 > 0$, and $L_1L_2 > L_3$, then according to the Routh–Hurwitz criteria, it is locally asymptotically stable.

Next, we focus on the Hopf bifurcation of the system (2.2) near P_4. Assuming that system (2.2) is locally asymptotically stable, while there exists $k = k^H$ such that $L_1(k^H)L_2(k^H) - L_3(k^H) = 0$, then Eq. (3.15) can be rewritten as:

$$(\lambda^2 + L_2)(\lambda + L_1) = 0. \tag{3.16}$$

Clearly, Eq. (3.16) has one real root $\lambda_1 = -L_1$ and two imaginary roots $\lambda_{2,3} = \pm i\sqrt{L_2}$. Now, rewriting the roots of the characteristic equation (3.16), while taking k as a bifurcation parameter as follows:

$$\lambda_1(k) = \varphi(k) + i\beta(k), \quad \lambda_2(k) = \varphi(k) - i\beta(k), \quad \lambda_3(k) = L_1.$$

Substituting the value of $\lambda_j(k) = \varphi(k) + i\beta(k)$ into the characteristic equation (3.16) yields the following result:

$$(\varphi(k) + i\beta(k))^3 + L_1(\varphi(k) + i\beta(k))^2 + L_2(\varphi(k) + i\beta(k)) + L_3 = 0. \tag{3.17}$$

Differentiating (3.17) with respect to k, gives:

$$N_1(k)\frac{\partial \varphi}{\partial k} - N_2(k)\frac{\partial \beta}{\partial k} = \Theta_1(k), \quad N_2(k)\frac{\partial \varphi}{\partial k} + N_1(k)\frac{\partial \beta}{\partial k} = \Theta_2(k), \tag{3.18}$$

where

$$N_1 = 3\varphi^2 - 3\beta^2 + 2L_1\varphi + L_2, \ \ N_2 = 6\varphi\beta + 2L_1\beta,$$
$$\Theta_1 = \beta^2\frac{\partial L_1}{\partial k} - \varphi^2\frac{\partial L_1}{\partial k} - \varphi\frac{\partial L_2}{\partial k} - \frac{\partial L_3}{\partial k}, \ \ \Theta_2 = 2\varphi\beta\frac{\partial L_1}{\partial k} + \beta\frac{\partial L_2}{\partial k}.$$

Noting that $\varphi(k^H) = 0$, $\beta(k^H) = \sqrt{L_2}$, we have $N_1(k^H) = -2L_2$, $N_2(k^H) = 2L_1\sqrt{L_2}$, $\Theta_1 = L_2\frac{\partial L_1}{\partial k} - \frac{\partial L_3}{\partial k}$, $\Theta_2 = \sqrt{L_2}\frac{\partial L_2}{\partial k}$. Now, let us check the transversality condition shown below:

$$\frac{\partial}{\partial k}(\mathrm{Re}\lambda(k))\bigg|_{k=k^H} = \frac{N_1\Theta_1 + N_2\Theta_2}{N_1^2 + N_2^2} \neq 0, \text{if } N_1\Theta_1 + N_2\Theta_2 \neq 0.$$

In other words, the bifurcation condition is satisfied and the system (2.2) undergoes a Hopf bifurcation at $k = k^H$.

Theorem 9 *The system* (2.2) *is locally asymptotically stable around the interior equilibrium* P_3 *if* $L_1 > 0, L_3 > 0, L_1L_2 > L_3$ *and unstable if* $L_3 < 0$. *When the system* (2.2) *has local asymptotic stability, then it undergoes a Hopf bifurcation around the coexistence equilibrium* P_4 *at* $k = k^H$ *such that* $L_1L_2 = L_3$ *given* $N_1\Theta_1 + N_2\Theta_2 \neq 0$.

Remark 3 Similarly, we can also consider σ, B, ρ or others as the bifurcation parameter. In this section, we choose k as the bifurcation parameter to analyze the Hopf bifurcation of the system (2.2) around P_4. The analysis of Hopf bifurcations with respect to other parameters will be presented in Sect. 4.

3.3.2 Delayed case

The dynamics of the boundary equilibrium points in the delayed system (2.3) are the same as (2.2). Therefore, we only consider the coexistence fixed point P_4. We linearize the system (2.3) as follows before exploring the dynamics near P_4:

$$\frac{d}{dt}\begin{pmatrix} X \\ Y_1 \\ Y_2 \end{pmatrix} = \begin{pmatrix} I_1 & D_{12} & D_{13} \\ D_{21} & D_{22} & D_{23} \\ D_{31} & D_{32} & 0 \end{pmatrix} + \begin{pmatrix} I_2 & 0 & 0 \\ 0 & 0 & 0 \\ 0 & 0 & 0 \end{pmatrix} \begin{pmatrix} X(t-\tau) \\ Y_1(t-\tau) \\ Y_2(t-\tau) \end{pmatrix},$$

here the parameters $D_{ij}(i \text{ or } j = 1, 2, 3)$ definitions are the same as before and

$$I_1 = -d_1 - \frac{s_1y_1^*(1 + y_1^*)}{(1 + x^* + y_1^*)^2} - \frac{s_2y_1^*(1 + \rho\alpha B)}{(1 + \rho\alpha B + x^*)^2}, \ \ I_2 = re^{-k(y_1^* + y_2^*)}\left(1 - \frac{2x^*}{V}\right).$$

The characteristic equation is obtained by performing calculations as follows:

$$\begin{vmatrix} I_1 + I_2 e^{-\lambda\tau} - \lambda & D_{12} & D_{13} \\ D_{21} & D_{22} - \lambda & D_{23} \\ D_{31} & D_{32} & -\lambda \end{vmatrix} = 0.$$

That is:

$$\lambda^3 + \Upsilon_1\lambda^2 + \Upsilon_2\lambda + (\Upsilon_3\lambda - \Upsilon_4\lambda^2 + \Upsilon_5)e^{-\lambda\tau} + \Upsilon_6 = 0, \tag{3.19}$$

where $\Upsilon_1 = -I_1 - D_{22}, \Upsilon_2 = I_1D_{22} - D_{23}D_{32} - D_{13}D_{31} - D_{12}D_{21}, \Upsilon_3 = I_2D_{22}, \Upsilon_4 = I_2, \Upsilon_5 = I_2D_{23}D_{32}, \Upsilon_6 = I_1D_{23}D_{32} + D_{13}D_{31}D_{22} - D_{12}D_{23}D_{31} - D_{21}D_{32}D_{13}$.

Take τ as the bifurcation parameter and let $\lambda(\tau) = \varphi(\tau) \pm i\beta(\tau)$ as the root of (3.19). By substituting $\lambda(\tau) = \varphi(\tau) \pm i\beta(\tau)$ into (3.19) and separating the real and imaginary parts from both sides gives:

$$\begin{aligned} &\varphi^3 - 3\varphi\beta^2 + \Upsilon_1(\varphi^2 - \beta^2) + \Upsilon_2\varphi + \Upsilon_6 + [(\Upsilon_3\varphi - \Upsilon_4\varphi^2 + \Upsilon_4\beta^2 \\ &\qquad + \Upsilon_5)\cos(\beta\tau) + (\Upsilon_3\beta - 2\Upsilon_4\varphi\beta)\sin(\beta\tau)]e^{-\varphi\tau} = 0, \end{aligned} \tag{3.20}$$

$$\begin{aligned} &-\beta^3 + 3\beta\varphi^2 + 2\Upsilon_1\varphi\beta + \Upsilon_2\beta + [(\Upsilon_3\beta - 2\Upsilon_4\varphi\beta)\cos(\beta\tau) \\ &\qquad -(\Upsilon_3\varphi - \Upsilon_4\varphi^2 + \Upsilon_4\beta^2 + \Upsilon_5)\sin(\beta\tau)]e^{-\varphi\tau} = 0. \end{aligned} \tag{3.21}$$

Setting $\varphi = 0$, Eqs. (3.20) and (3.21) are written as:

$$-\Upsilon_1\beta^2 + \Upsilon_6 + (\Upsilon_4\beta^2 + \Upsilon_5)\cos(\beta\tau) + \Upsilon_3\beta\sin(\beta\tau) = 0, \tag{3.22}$$

$$-\beta^3 + \Upsilon_2\beta + \Upsilon_3\beta\cos(\beta\tau) - (\Upsilon_4\beta^2 + \Upsilon_5)\sin(\beta\tau) = 0. \tag{3.23}$$

Eliminating τ by squaring both sides of (3.20) and (3.21) and adding them together, we have:

$$\beta^6 + (\Upsilon_1\beta^2 - \Upsilon_6)^2 - (\Upsilon_4\beta^2 - \Upsilon_5)^2 - (\Upsilon_3\beta)^2 = 0. \tag{3.24}$$

Let $\Psi(\beta) = \beta^6 + (\Upsilon_1\beta^2 - \Upsilon_6)^2 - (\Upsilon_4\beta^2 - \Upsilon_5)^2 - (\Upsilon_3\beta)^2$ and $\lim_{\beta\to\infty}\Psi(\beta) = \infty$. If $\beta = 0$ then $\Psi(\beta) = \Upsilon_6^2 - \Upsilon_5^2$. Therefore, (3.24) has at least one and at most three positive roots under the condition $\Upsilon_6^2 - \Upsilon_5^2 < 0$. Any solution $\beta_i, i = 1, 2, 3$ in (3.24) can be matched with a corresponding solution τ_i as follows in (3.22):

$$\tau_i = \frac{1}{\beta_i}\cos^{-1}\left(\frac{(\Upsilon_4\beta_i^2 + \Upsilon_5)(\Upsilon_1\beta_i^2 - \Upsilon_6) + \Upsilon_3\beta_i^4}{(\Upsilon_4\beta_i^2 + \Upsilon_5)^2 + (\Upsilon_3\beta_i)^2}\right) + \frac{2j\pi}{\beta_i}, i = 1, 2, 3, j = 0, 1, 2\cdots.$$

Let $\tau^H = \min\tau_i$, then according to Butler's lemma [41] it is known that the system (2.3) remains stable for $0 < \tau_i < \min\tau^H$ and becomes unstable for $\tau_i > \min\tau^H$. Now, we check

the transversality criterion $\frac{\partial}{\partial\tau}(\mathrm{Re}\lambda(\tau))\big|_{\tau=\tau^H}$. Differentiating (3.20) and (3.21) with respect to τ and substituting $\varphi = 0$, we have

$$N_3\frac{\partial\varphi}{\partial\tau} + N_4\frac{\partial\beta}{\partial\tau} = \Theta_3, \tag{3.25}$$

$$-N_4\frac{\partial\varphi}{\partial\tau} + N_3\frac{\partial\beta}{\partial\tau} = \Theta_4, \tag{3.26}$$

where

$$\begin{aligned}
N_3 = &-3\beta^2 + \Upsilon_2 - \tau\left(\Upsilon_4\beta^2 + \Upsilon_5\right)\cos(\beta\tau) - \tau\Upsilon_3\beta\sin(\beta\tau) + \Upsilon_3\cos(\beta\tau)\\
&- 2\Upsilon_4\beta\sin(\beta\tau),\\
N_4 = &-2\Upsilon_1 + 2\Upsilon_4\cos(\beta\tau) - \tau\left(\Upsilon_4\beta^2 + \Upsilon_5\right)\sin(\beta\tau) + \Upsilon_3\sin(\beta\tau) + \tau\Upsilon_3\beta\cos(\beta\tau),\\
\Theta_3 = &\beta\left(\Upsilon_4\beta^2 + \Upsilon_5\right)\sin(\beta\tau) - \Upsilon_3\beta^2\cos(\beta\tau), \Theta_4 = \beta\left(\Upsilon_4\beta^2 + \Upsilon_5\right)\sin(\beta\tau)\\
&+ \Upsilon_3\beta^2\cos(\beta\tau).
\end{aligned}$$

Eliminating $\frac{\partial\beta}{\partial\tau}$ through (3.25) and (3.26) yields results in terms of $\frac{\partial\varphi}{\partial\tau}$ as follows:

$$\frac{\partial\varphi}{\partial\tau}(\mathrm{Re}\lambda(\tau)) = \frac{N_3\Theta_3 - N_4\Theta_4}{N_3^2 + N_4^2}. \tag{3.27}$$

If (3.27) satisfies the condition $N_3\Theta_3 - N_4\Theta_4 > 0$, then

$$\frac{\partial\varphi}{\partial\tau}(\mathrm{Re}\lambda(\tau))\bigg|_{\tau=\tau^H} = \frac{N_3\left(\tau^H\right)\Theta_3\left(\tau^H\right) - N_4\left(\tau^H\right)\Theta_4\left(\tau^H\right)}{N_3^2\left(\tau^H\right) + N_4^2\left(\tau^H\right)} > 0.$$

Regarding the stability with respect to the parameter τ and the Hopf bifurcation condition of the system (2.3), we summarize as follows:

Theorem 10 *For the system* (2.3), *with the interior equilibrium point* P_4:

(1) *There exists* $\tau = \tau^H$ *such that the system* (2.3) *is locally asymptotically stable near* P_4 *for* $0 < \tau < \tau^H$ *and becomes unstable when* $\tau > \tau^H$.

(2) *Furthermore, the system* (2.3) *will undergo a Hopf bifurcation at* P_4 *when* $\tau = \tau^H$, *given that* $N_3\Theta_3 - N_4\Theta_4 > 0$.

4 Numerical simulation

In this section, we provide some biological interpretations and numerical simulations to explore and demonstrate the impact of various parameter variations on the system. Our numerical simulations involve use the ode23 solver in MATLAB to solve the differential equation and partly utilize Matcont [42]. To achieve this, we select the following parameters for numerical simulations.

$$\begin{aligned}
&r = 1.2, k = 0.5, V = 10, d_1 = 0.1, s_1 = 0.6, \rho = 0.1, \alpha = 0.15, B = 2,\\
&\varpi_1 = 0.9, d_2 = 0.2, s_2 = 0.4, \varpi_2 = 0.8, \delta = 0.05, c = 0.1, \sigma = 0.3.
\end{aligned} \tag{4.1}$$

Next, we will observe the behavior of the system (2.2) or (2.3) by varying certain parameters in (4.1) to explore the impact of different factors on the system. We begin by exploring

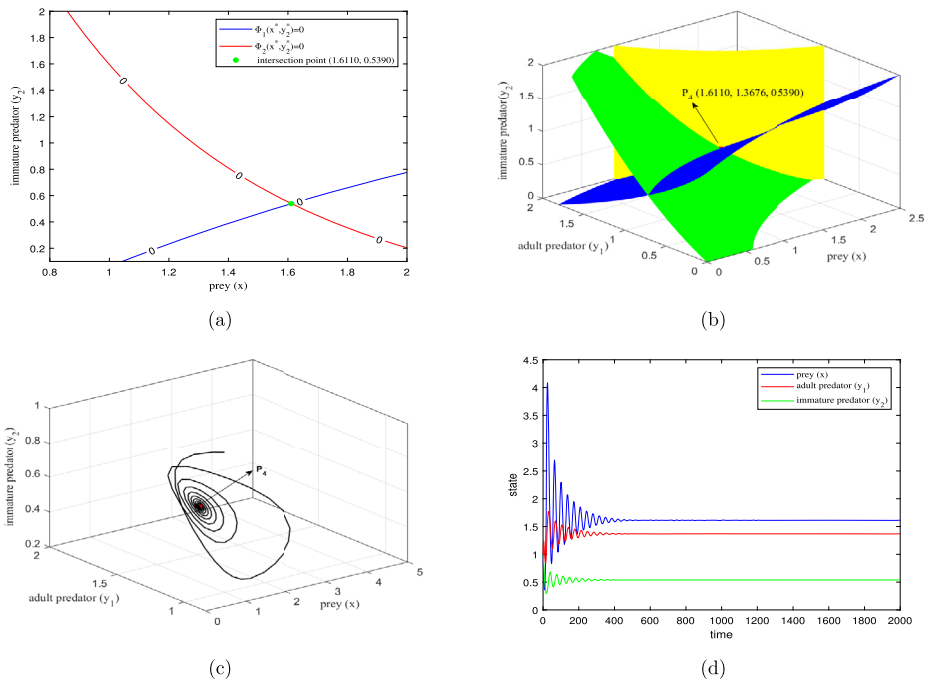

Figure 2 Stable nature of $P_4(1.6110, 1.3676, 0.5390)$ of the system (2.2) under the parameter set (4.1). Here, (a) is existence of the intersection point of the nullclines $\Phi_1(x^*, y_2^*) = 0$ and $\Phi_2(x^*, y_2^*) = 0$ in the $x - y_2$ plane, (b) is the existence of interior equilibrium in the $x - y_1 - y_2$ space, (c) is the phase graph, (d) is the time curves with $x(0) = y_1(0) = y_2(0) = 1$

some fundamental features of (4.1) within the system (2.2) without time delay, including equilibrium point and stability states.

4.1 Nondelay system

The parameter set (4.1) yields the equilibrium point $P_4 = (1.6110, 1.3676, 0.5390)$ for the system (2.2) by plotting nullclines as shown in Figs. 2(a) and (b). Figures 2(c) and (d) illustrate that the current parameter set (4.1) enables the system (2.2) to maintain a stable state. Equilibrium points indicate the stable or long-term behavior a system may attain given specific conditions. Thus, sensitivity analysis of equilibrium points in dynamic systems is of great significance in research. It helps us understand how the system's behavior and stability change under different parameter conditions. By analyzing the system's response to parameter variations, we can identify the key parameters that have the most significant impact on system performance, thereby optimizing these parameters to enhance performance and stability. Here, we use partial rank correlation coefficients (PRCCs) to study the sensitivity of system coexistence equilibrium points. The parameters k, σ, δ, and B are considered as input parameters, and the output variables x^*, y_1^*, and y_2^* are determined through (3.2), then based on the parameter set (4.1) we plot Fig. 3. From Fig. 3, it is observed that prey are most sensitive to fear and have a positive impact in internal equilibrium, while immature predator similarly respond to additional food. The adult rate has a positive effect on prey and adult predator but has a negative impact on immature predator. The internal equilibrium shows a lack of significant sensitivity to cooperation among predators.

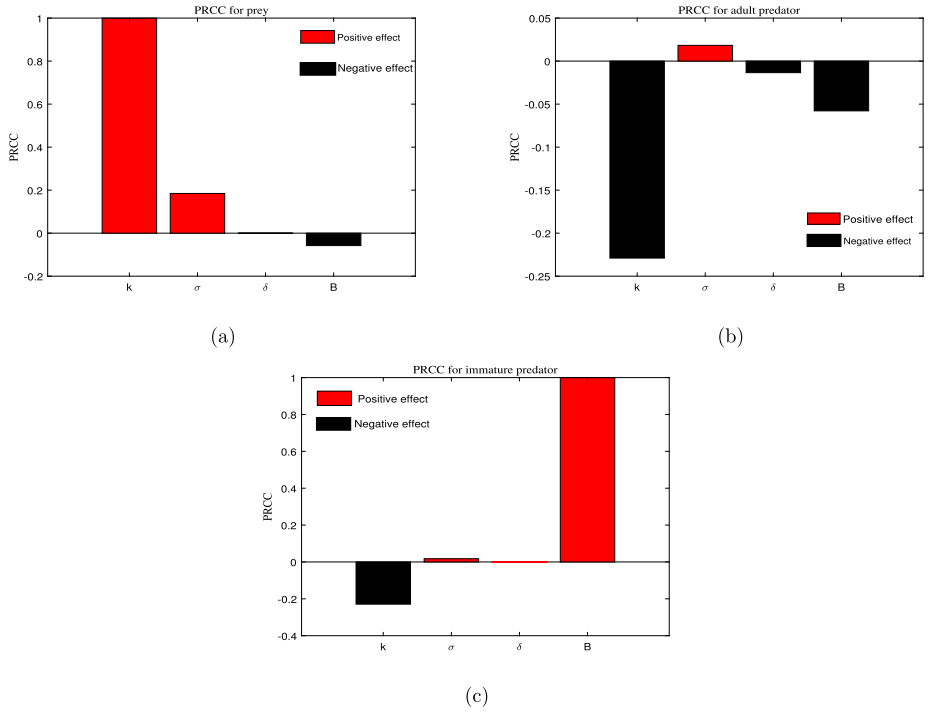

Figure 3 Analyzing the sensitivity of parameters relative to (4.1) for the prey, adult, and immature predator

(1) Effect of fear

We focus on exploring the impact of fear on populations. The parameter k represents the level of fear that influences the birth rate of prey. First, we observe how changes in the fear parameter k affect the stability of the system (2.2), then extend the parameter k in (4.1) in two opposite directions and record the temporal state diagrams at $k' = 0.4$ and $k'' = 1.5$ as shown in Figs. 4(a) and (b). In Fig. 4, the transition from (a) to (b) shows a shift in the system's equilibrium point from an internal equilibrium point to an immature predator-free equilibrium point. By comparing Figs. 2(c) and (d), we can infer that the system's state has changed from stable to unstable. According to bifurcation theory, it is known that changes in the system may be accompanied by bifurcations, and this result has been validated in the process of numerical simulation (see Figs. 4(c) and (d)). Figure 4(c) displays the equilibrium points steady state and bifurcations in the $y_2 - k$ plane related to the parameter k by Matcont. It demonstrates that when the value of k is small, the equilibrium-point type of the system (2.2) is an internal equilibrium point. When k reaches $k^S = 1.4156722$, it undergoes a transcritical bifurcation (BP), resulting in the disappearance of immature predator and the system's equilibrium point transitions to a predator-free equilibrium point. Before transitioning to the predator-free equilibrium point, k undergoes a subcritical Hopf bifurcations (H) around the internal equilibrium point at $k^H = 0.46426044$ (see Fig. 4(d)). Figure 4 demonstrate a substantial impact on the system dynamics due to the prey of fear.

(2) Effect of adult rate

Now, we observe how the system (2.2) stability changes with variations in the adult rate σ. Similar to before, we extend the parameter σ from the center with $\sigma = 0.3$ as the midpoint towards both ends. It is observed that the system (2.2) steady states occur

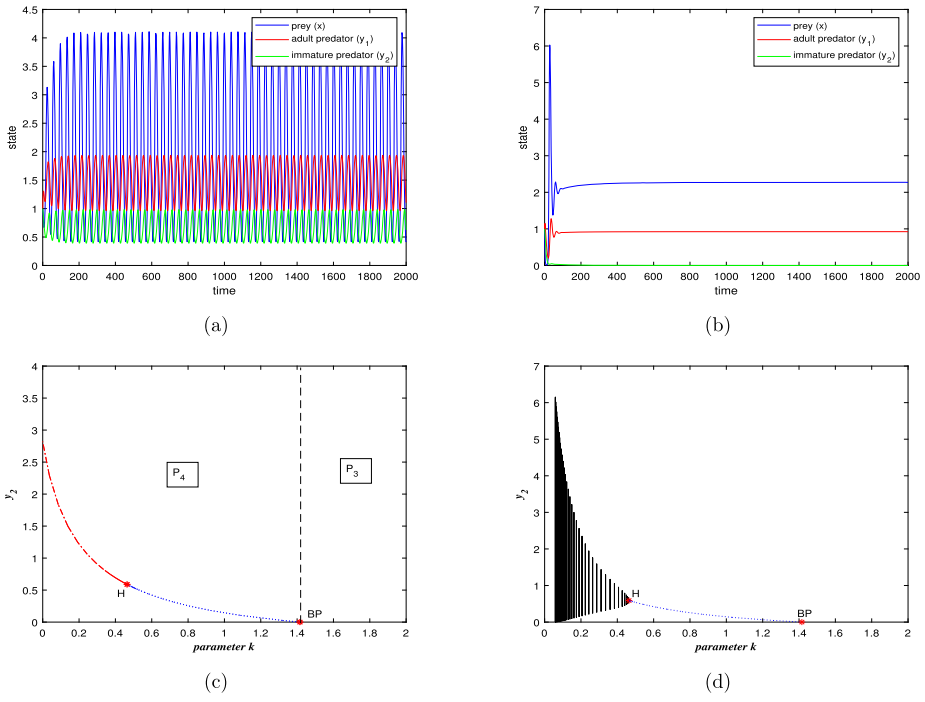

Figure 4 The analysis of the impact of fear (k) on relevant graphs. Here, (a) is the time-series graph of (2.2) with $k' = 0.4$ and (b) with $k'' = 1.5$, (c) is the steady state of equilibrium points and bifurcation thresholds, where the red dashed line represents instability, the blue dashed line represents stability, and P_3 and P_4 are types of equilibrium points. (d) is the Hopf bifurcation and limit cycles

when $\sigma' = 0.25$ and $\sigma'' = 0.45$, as shown in Figs. 5(a) and (b). In Fig. 5(a), the system's steady state has changed compared to Fig. 2(d), while the types of equilibrium points remain unchanged. Conversely, in Fig. 5(b), both the steady states and equilibrium-point types have changed compared to Fig. 5(d). This process may occur for a Hopf bifurcation (H) or a transcritical bifurcation (BP) (see Figs. 5(c) and (d)). The system shows a Hopf bifurcation at $\sigma^H = 0.29236512$ as the maturation rate of immature predator gradually rises, followed by a transcritical bifurcation at $\sigma^S = 0.36970317$. Comparing with Fig. 4, it is evident that the parameter σ has a similar influence to k in the system.

(3) Effect of predator cooperation

In the absence of predator cooperation ($\delta' = 0$), the system state observed in Fig. 6(a) indicates the extinction of immature predator. On the other hand, the cooperation rate among predators exhibits periodic oscillations in the system when $\delta'' = 0.1$ (see Fig. 6(b)). Similar to the previous analysis, we understand that undergoes a transcritical bifurcation (BP) from the stable state (Fig. 2(b) to Fig. 6(a)), and subsequently experiences a Hopf bifurcation (H) in Fig. 6(b)) (see Figs. 6(c) and (d)). In Figs. 6(c) and (d), parameter δ undergoes a BP bifurcation at $\delta^S = 0.0085786992$ and an H bifurcation at $\delta^H = 0.05411523$, respectively.

(4) Effect of additional food

First, consider the system state without additional food ($B' = 0$) and record in Fig. 7(a), then the system achieves a stable equilibrium. We observe that the system exhibits periodic oscillations when we set $B'' = 4$ (see Fig. 7(b)). In Fig. 7(c), the system's equilibrium

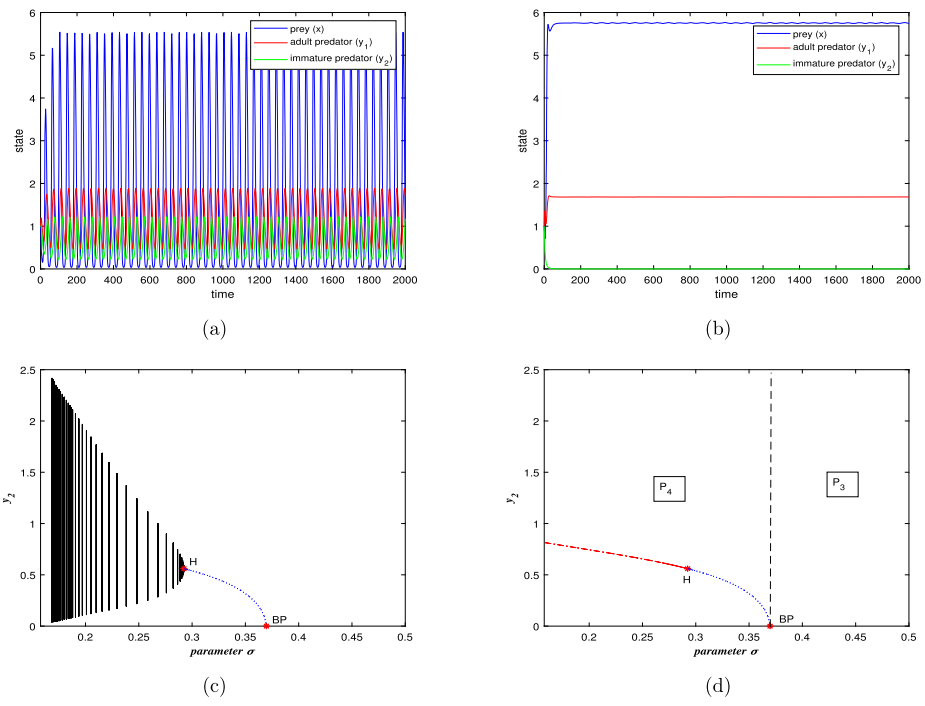

Figure 5 The analysis of the maturation rate (σ) on relevant graphs. Here, (a) is the time-series graph of (2.2) with $\sigma' = 0.25$ and (b) is $\sigma'' = 0.45$, (c) is the Hopf bifurcation and limit cycles, (d) is the steady state of equilibrium points and bifurcation thresholds, where the red dashed line represents instability, the blue dashed line represents stability, and P_4 and P_3 are types of equilibrium points

points and bifurcation thresholds are plotted, and it is observed that a Hopf bifurcation occurs at $B = 2.5417534$, leading to the emergence of periodic oscillations, as shown in Fig. 7(d). Figure 7(c) demonstrates that providing additional food appropriately can help maintain the system stability and it is detrimental to the prey population but beneficial to the predator population.

In the previous section, we explored the impact of additional food on biological populations. Next, we will investigate whether additional food has an effect on other factors such as fear. To understand the impact of additional food on fear, we plot the equilibrium states of the fear parameter k at different levels of additional food (B) in Fig. 7(e). It demonstrates that without additional food, the growth of the immature predator population is more adversely affected under high levels of fear compared to when additional food is available. Conversely, under lower levels of fear, the presence of additional food suppresses the growth of the immature predator population. This highlights the essential role of providing additional food to predators in mitigating the fear effect. In Fig. 7(e), we solely observe the variation of the fear parameter k under the fixed condition of the additional food parameter B. If both parameters B and k are altered, the dynamics of the system may become more complex while also richer. Hence, our subsequent endeavor involves investigating the bifurcation structure of the system (2.2) as two parameters undergo variations.

4.2 Two-parameter bifurcation

• Space of two parameters B and k

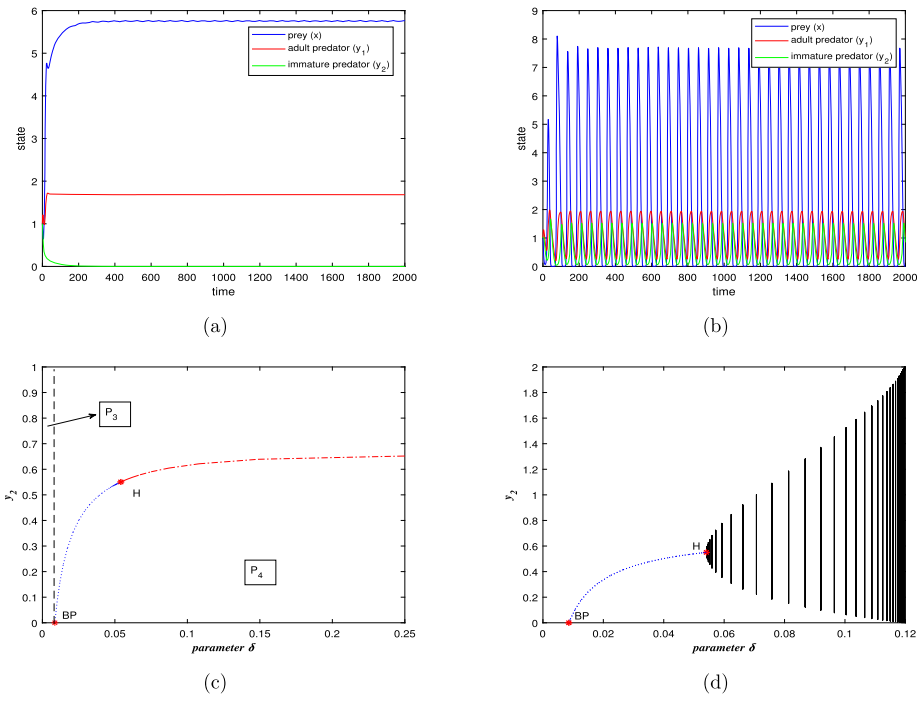

Figure 6 The analysis of the impact of cooperation rate (δ) on relevant graphs. Here, (a) is the time-series graph of (2.2) with $\delta' = 0.4$ and (b) is $\delta'' = 1.5$, (c) is the steady state of equilibrium points and bifurcation thresholds, where the red dashed line represents instability, the blue dashed line represents stability, P_3 and P_4 are types of equilibrium points. (d) is the Hopf bifurcation and limit cycles

For a clearer grasp of how fear effect k and additional food B dynamically interact, we plot a two-parameter bifurcation analysis within the $B-k$ plane as Fig. 8. In Fig. 8, the $B-k$ space is divided into three parts denoted as R_i $i = 1, 2, 3$, respectively. When the value of k is large, the system resides in the R_3 region, which represents a stable coexistence equilibrium state. As the value of k decreases, the system enters the R_2 region between the Hopf-bifurcation curve and the saddle-node bifurcation of the limit cycle (LPC) curve, where the system transitions from locally asymptotically stable coexistence to coexistence with periodic oscillations. Finally, when the value of k is very small and the appearance of additional food leads to prey extinction (in the region to the right of (R_1)). When both k and B increase simultaneously to the upper-right corner of R_1, the system reaches a state of coexistence with periodic oscillations.

• Space of two parameters B and σ

Similar to before, we graph two-parameter bifurcations in the $B-\sigma$ plane. In Fig. 9, with the increase of both B and σ, a generalized Hopf point GH (8.4679187, 0.40431804) and a Bogdanov–Takens point BT (8.8302929, 0.41328949) appear successively. During the process of drawing the saddle-node bifurcation of the limit cycle (LPC) from the GH point, a Period Doubling bifurcation point PD (4.1274303, 0.25342062) appears simultaneously, leading to the emergence of coexistence oscillation region (R_1) and prey-extinction region (R_4). During the process of plotting the saddle-node bifurcation (LP) from the BT point, the first Cusp bifurcation piont CP_1 occurs at position (9.4288472, 0.42509151), followed by another CP_2 at (3.0630065, 0.37653808). The LP curve delineates the coexistence local

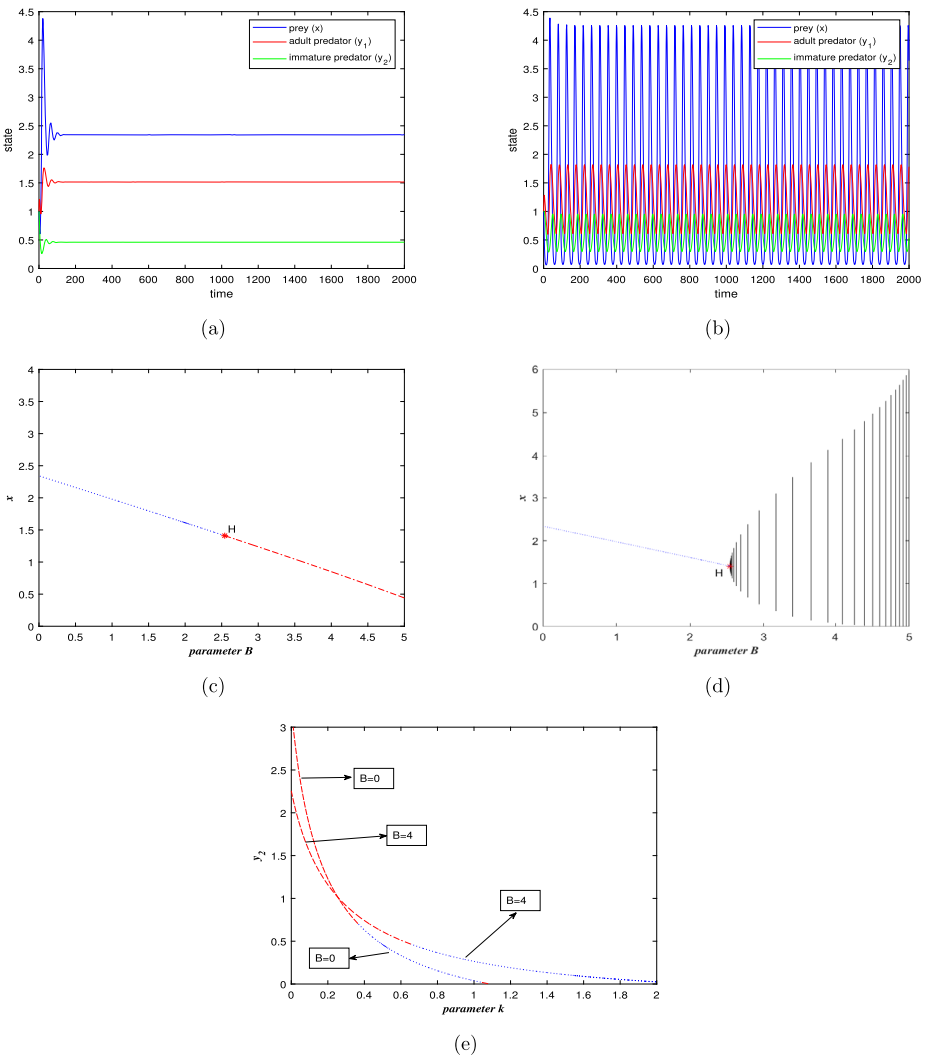

Figure 7 The analysis of the impact of additional food (B) on relevant graphs. Here, (a) is the time-series graph of (2.2) with $B' = 0$ and (b) is $B'' = 4$, (c) is the steady state of equilibrium points and bifurcation thresholds, where the red dashed line represents instability, the blue dashed line represents stability, (d) is the Hopf bifurcation and limit cycles and (e) is the effect of different values of k on population growth under varying conditions of B

asymptotically stability region (R_2) from the immature predator-free stability region (R_3).

4.3 Delayed system

(1) Time-delay dynamics and its interaction with additional food

In the preceding simulation subsection, we examined the interplay between fear and additional food. In this subsection, we also analyze the impact of time delay across various scenarios involving additional food. This approach allows us to not only comprehend the effects of time delay but also to investigate the interaction between additional food and time delay.

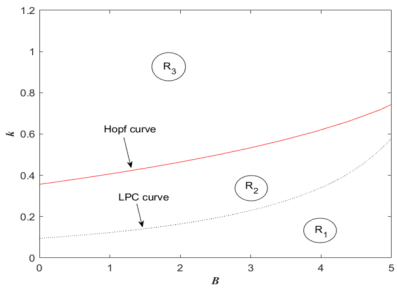

Figure 8 The bifurcation diagram for B and k parameters

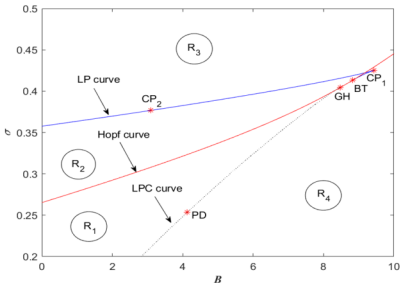

Figure 9 The bifurcation diagram for B and σ parameters

Figures 2(d) and 7(a) clearly demonstrate that the system without delay is locally asymptotically stable for values of $B = 0$ or 2. In parameter set (4.1), we examine $B = 0$ and 2 separately, and observe that the system states in the delayed system (2.3) with a delay of $\tau = 0.4$ are both locally asymptotically stable, as illustrated in Figs. 10(a) and (b). However, when the delay is increased to $\tau = 3$, the system becomes unstable, as shown in Fig. 10(c). During the transition of the system's steady states, Hopf bifurcations occur at $\tau = 2.5455$ and 0.5152 under the conditions where $B = 0$ and 2, respectively (see Figs. 10(e) and (f)). To further elucidate the relationship between additional food and delay, we present the $B - \tau$ bifurcation plane in Fig. 11. In this figure, the bifurcation curve declines as B increases, effectively dividing the $B - \tau$ plane into a stable region (R_1) and an unstable region (R_2).

5 Conclusions

In this paper, we present a stage-structured predator–prey mathematical model that incorporates the effects of fear, additional food, and predator cooperation. The development of the mathematical model relies on the integration of Holling Type-II and Beddington–DeAngelis-type functional responses for prey within predator–prey interactions. Initially, we demonstrate that there are specific parameter constraints under which all solutions remain positive and uniformly bounded. Following this, we analyze various types of equilibrium points in the system and their conditions for existence. With respect to equilibrium points, we employ Lyapunov stability theory and the Jacobian matrix to examine the conditions for local asymptotic stability around each equilibrium point. Additionally, we utilize bifurcation theory to investigate bifurcations occurring near certain equilibrium points.

Finally, we explore the system's dynamics from a numerical perspective, examining how factors such as fear, maturation rate, cooperation, additional food, and delay lead to Hopf bifurcations or transcritical bifurcations that result in changes in equilibrium types. Furthermore, we investigate the relationship between additional food and two other factors:

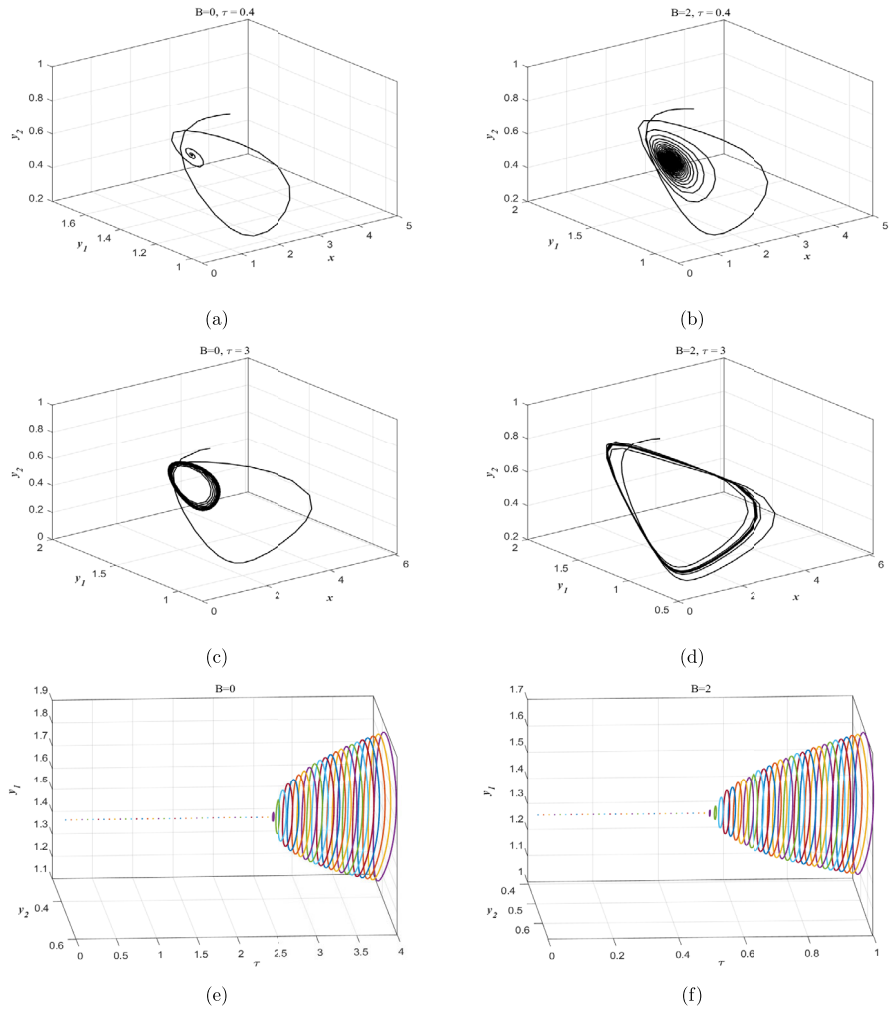

Figure 10 The analysis of the impact of delay (τ) on relevant graphs. Here, (a) is the phase graph of (2.2) with $B = 0, \tau = 0.4$, (b) is $B = 2, \tau = 0.4$, (c) is $B = 0, \tau = 3$, (d) is $B = 2, \tau = 3$, (e) is the Hopf bifurcation picture for $\tau \in [0, 4]$ under $B = 0$, and (f) is $\tau \in [0, 1]$ under $B = 2$

Figure 11 The bifurcation diagram for B and τ parameters

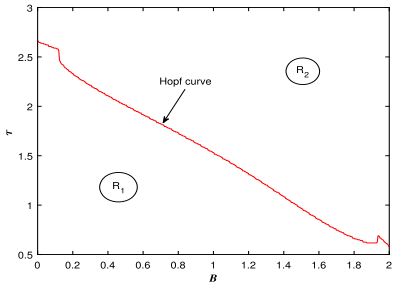

fear and delay. Through this analysis, we delve into the more complex two-parameter bifurcations involving additional food and other factors, such as Hopf, saddle-node, period-doubling, cusp bifurcation, and Bogdanov-Taken bifurcations, which reveal intricate and

diverse dynamics. After conducting a series of theoretical analyses and numerical simulations, we summarize the main conclusions as follows:

- A stage-structured predator–prey mathematical model is developed, incorporating the effects of predator-induced fear on prey-population growth, as well as variations in cooperation and age structure among predators, where immature predators are provided with additional food.
- Low levels of fear can induce cyclic oscillations in the system, while an appropriate level of fear can stabilize it. However, excessive levels of fear may indirectly harm predators, potentially leading to the extinction of immature predators (refer to Fig. 4(c)).
- The adult rate of immature predator individuals significantly influences the age structure of the population. A lower adult rate among immature individuals may result in a higher proportion of immatures within the population, potentially causing an imbalance in population structure that impacts the ecological function of the community. Conversely, a high adult rate may also disadvantage the population size of juveniles.
- Fig. 6 illustrates that cooperative behavior among predators enhances the growth of immature predators. From an ecological standpoint, populations of each species generally exhibit stability when predator cooperation is minimal; however, they experience significant fluctuations over time when predator cooperation is pronounced.
- Providing supplementary food for immature predators can suppress the population growth of prey. An excessive supply of additional food may lead to system oscillations. It is essential to consider various factors, such as the level of fear, which can also influence the effects of the additional food (refer to Fig. 7(e)).
- The system inherently possesses a certain level of resilience to fear delay, but exceeding this capacity can result in stable changes. The introduction of additional food can mitigate the impact of fear delay, thereby enhancing the system's tolerance to delay (refer to Figs. 10(e) and (f) and Fig. 11).

In the complex and diverse natural world, we propose that future research should incorporate nonlinear mortality resulting from antipredator activities and stochastic environmental factors into the model to enhance its realism. Furthermore, we anticipate that applying the reaction–diffusion model [43, 44] and the infectious-disease model [45, 46] will yield interesting findings. However, these aspects will be reserved for further exploration in our future work.

Acknowledgements
The authors greatly appreciate the support from NSF of China, which enabled the completion of this study.

Author contributions
HM conducted all the analyses and wrote the initial draft of the manuscript. YS contributed to the conception of the study. All authors read and approved the final manuscript.

Funding
This work is supported by Science and Technology Program of Inner Mongolia Autonomous Region (Nos. 2023YFHH0024).

Data availability
Not applicable.

Declarations

Competing interests
The authors declare that they have no competing interests in this paper.

Received: 28 June 2024 Accepted: 12 January 2025 Published online: 03 February 2025

References

1. Lotka, A.J.: Elements of physical biology. Nature **116** (1925)
2. Volterra, V.: Variazioni e fluttuaziono del numero di individui in specie animali conviventi, Memoria della Reale Accademia Nazionale dei Linceii, vol. 2 (1926)
3. Holling, C.S.: Some characteristics of simple types of predation and parasitism. Can. Entomol. **91**(7), 385–398 (1959)
4. Beddington, J.R.: Mutual interference between parasites or predators and its effect on searching efficiency. J. Anim. Ecol. **44**(1), 331–340 (1975)
5. Mao, J.S., Boyce, M.S., Smith, D.W., Singer, F.J., Vales, D.J., Vore, J.M., Merrill, E.H.: Habitat selection by elk before and after wolf reintroduction in Yellowstone National Park. J. Wildl. Manag. **69**(4), 1691–1707 (2005)
6. Ripple, W.J., Larsen, E.J., Renkin, R.A., Smith, D.W.: Trophic cascades among wolves, elk and aspen on Yellowstone National Park's northern range. Biol. Conserv. **102**(3), 234 (2001)
7. Zanette, L.Y., White, A.F., Allen, M.C., Clinchy, M.: Perceived predation risk reduces the number of offspring songbirds produce per year. Science **334**, 1398–1401 (2011)
8. Wang, X., Zanette, L., Zou, X.: Modelling the fear effect in predator–prey interactions. J. Math. Biol. **73**(5), 1179–1204 (2016)
9. Václav, R., Hoi, H., Blomqvist, D.: Food supplementation affects extrapair paternity in house sparrows (Passer domesticus). Behav. Ecol. **14**(5), 730–735 (2003)
10. Wilson, W.E. Jr.: The effects of supplemental feeding on wintering black-capped chickadees (Poecile atricapilla) in central Maine: population and individual responses. Wilson Bull. **113**(1), 65–72 (2001)
11. Ghosh, J., Sahoo, B., Poria, S.: Prey-predator dynamics with prey refuge providing additional food to predator. Chaos Solitons Fractals **96**, 110–119 (2017)
12. Shao, Y.: Bifurcations of a delayed predator-prey system with fear, refuge for prey and additional food for predator. Math. Biosci. Eng. **20**(4), 7429–7452 (2023)
13. Thirthar, A.A., Majeed, S.J., Alqudah, M.A., Panja, P., Abdeljawad, T.: Fear effect in a predator–prey model with additional food, prey refuge and harvesting on super predator. Chaos Solitons Fractals **159**, 112091 (2022)
14. Ananth, V.S., Vamsi, D.K.K.: Achieving minimum-time biological conservation and pest management for additional food provided predator–prey systems involving inhibitory effect, a qualitative investigation. Acta Biotheor. **70**(1), 5 (2022)
15. Huang, C.Y., Zhao, M., Zhao, L.C.: Permanence of periodic predator–prey system with two predators and stage structure for prey. Nonlinear Anal., Real World Appl. **11**(1), 503–514 (2010)
16. Lu, W., Xia, Y., Bai, Y.: Periodic solution of a stage-structured predator-prey model incorporating prey refuge. Math. Biosci. Eng. **17**(4), 3160–3174 (2020)
17. Kaushik, R., Banerjee, S.: Predator–prey system with multiple delays: prey's countermeasures against juvenile predators in the predator–prey conflict. J. Appl. Math. Comput. **68**(4), 2235–2265 (2022)
18. Kundu, S., Maitra, S.: Dynamics of a delayed predator-prey system with stage structure and cooperation for preys. Chaos Solitons Fractals **114**, 453–460 (2018)
19. Kong, W., Shao, Y.: The effects of fear and delay on a predator-prey model with Crowley-Martin functional response and stage structure for predator. AIMS Math. **8**(12), 29260–29289 (2023)
20. Hinton, J.W., Chamberlain, M.J.: Space and habitat use by a red wolf pack and their pups during pup-rearing. J. Wildl. Manag. **74**(1), 55–58 (2010)
21. MacNulty, D.R., Tallian, A., Stahler, D.R., Smith, D.W.: Influence of group size on the success of wolves hunting bison. PLoS ONE **9**(11), e112884 (2014)
22. Enatsu, Y., Roy, J., Banerjee, M.: Hunting cooperation in a prey–predator model with maturation delay. J. Biol. Dyn. **18**(1), 2332279 (2024)
23. Vishwakarma, K., Sen, M.: Role of Allee effect in prey and hunting cooperation in a generalist predator. Math. Comput. Simul. **190**, 622–640 (2021)
24. Alves, M.T., Hilker, F.M.: Hunting cooperation and Allee effects in predators. J. Theor. Biol. **419**, 13–22 (2017)
25. Hu, D., Li, Y., Liu, M., Bai, Y.: Stability and Hopf bifurcation for a delayed predator–prey model with stage structure for prey and Ivlev-type functional response. Nonlinear Dyn. **99**, 3323–3350 (2020)
26. Kundu, S., Maitra, S.: Dynamical behaviour of a delayed three species predator–prey model with cooperation among the prey species. Nonlinear Dyn. **92**, 627–643 (2018)
27. Jang, S.R., Yousef, A.M.: Effects of prey refuge and predator cooperation on a predator–prey system. J. Biol. Dyn. **17**(1), 2242372 (2023)
28. Wu, D., Zhao, M.: Qualitative analysis for a diffusive predator–prey model with hunting cooperative. Phys. A, Stat. Mech. Appl. **515**, 299–309 (2019)
29. Pandey, S., Ghosh, U., Das, D., Chakraborty, S., Sarkar, A.: Rich dynamics of a delay-induced stage-structure prey–predator model with cooperative behaviour in both species and the impact of prey refuge. Math. Comput. Simul. **216**, 49–76 (2024)
30. Ramasamy, S., Banjerdpongchai, D., Park, P.: Stability and bifurcation analysis of delayed tri-trophic food chain model in poisoned environment with fear effect and additional food. Math. Methods Appl. Sci. (2023)
31. Dubey, B., Kumar, A.: Stability switching and chaos in a multiple delayed prey–predator model with fear effect and anti-predator behavior. Math. Comput. Simul. **188**, 164–192 (2021)
32. Shao, Y.: Fear and delay effects on a food chain system with two kinds of different functional responses. Int. J. Biomath. **17**(03), 2350025 (2024)
33. Sui, M., Du, Y.: Bifurcations, stability switches and chaos in a diffusive predator-prey model with fear response delay. Electron. Res. Arch. **31**(9), 5124–5150 (2023)

34. Yang, R., Ren, H., Cheng, X.: A diffusive predator-prey system with prey refuge and gestation delay. Adv. Differ. Equ. **2017**, 158 (2017)
35. Wang, Y., Zou, X.: On a predator–prey system with digestion delay and anti-predation strategy. J. Nonlinear Sci. **30**(4), 1579–1605 (2020)
36. Tian, B., Qiu, Y., Chen, N.: Periodic and almost periodic solution for a non-autonomous epidemic predator-prey system with time-delay. Appl. Math. Comput. **215**(2), 779–790 (2009)
37. Mondal, S., Maiti, A., Samanta, G.P.: Effects of fear and additional food in a delayed predator–prey model. Biophys. Rev. Lett. **13**(04), 157–177 (2018)
38. Das, A., Samanta, G.P.: Modeling the fear effect on a stochastic prey–predator system with additional food for the predator. J. Phys. A, Math. Theor. **51**(46), 465601 (2018)
39. Yang, X., Chen, L., Chen, J.: Permanence and positive periodic solution for the single-species nonautonomous delay diffusive models. Comput. Math. Appl. **32**(4), 109–116 (1996)
40. Perko, L.: Differential Equations and Dynamical Systems. Springer, New York (2001)
41. Freedman, H., Rao, V.S.H.: The trade-off between mutual interference and time lags in predator-prey systems. Bull. Math. Biol. **45**(6), 991–1004 (1983)
42. Dhooge, A., Govaerts, W., Kuznetsov, Y.A., Meijer, H.G.E., Sautois, B.: New features of the software MatCont for bifurcation analysis of dynamical systems. Math. Comput. Model. Dyn. Syst. **14**(2), 147–175 (2008)
43. Zhang, H., Qi, H.: Hopf bifurcation analysis of a predator–prey model with prey refuge and fear effect under non-diffusion and diffusion. Qual. Theory Dyn. Syst. **22**(4), 135 (2023)
44. Yang, R., Zhao, X., An, Y.: Dynamical analysis of a delayed diffusive predator–prey model with additional food provided and anti-predator behavior. Mathematics **10**(3), 469 (2022)
45. He, X., Liu, M., Xu, X.: Analysis of stochastic disease including predator-prey model with fear factor and Lévy jump. Math. Biosci. Eng. **20**, 1750–1773 (2023)
46. Zhang, C., Liu, S., Huang, J., Wang, W.: Stability and Hopf bifurcation in an eco-epidemiological system with the cost of anti-predator behaviors. Math. Biosci. Eng. **20**(5), 8146–8161 (2023)

Publisher's Note